Gravitational Waves in Cosmology

Student Seminar '09 Report

of

Michael Agathos

February 26, 2009

Supervisors:
Prof. T. Prokopec
J. F. Koksma

Utrecht University
Faculty of Physics and Astronomy
Institute of Theoretical Physics

Contents

1 Introduction

The story of Gravitational Waves begins in 1916, very shortly after the formulation of General Relativity. As taught by earlier classical field theories, such as Electromagnetism, physicists felt the urge to look for radiative solutions of the Einstein equations. This kind of wave-like propagating solutions would be the gravitational equivalent of the EM waves.

But this was a far from trivial task. The highly non-linear nature of the 2nd order differential equations required a different and more careful approach, which also had conceptual implications. However the landscape of this fascinating field was soon clarified and a consistent theory of GWs was formulated in a few years time.

In this project we will deal with gravitational waves that emerge from processes of cosmological scales during the early stages of evolution of the Universe, according to the modern standard cosmological model. In times when the matter and energy content of the whole Universe was confined in a tiny volume and temperatures of $10^{32}K$ where typical, extremely violent macroscopic processes occurred providing sources of gravitational radiation strong enough to comprise relics of this epoch, that could even be detectable at present time experiments.

However, no gravitational wave detection experiment has been essentially successful up to today, meaning of course that no gravitational waves have been detected yet, in spite of the variety of sources predicted by several theoretical calculations. These include not only sources of cosmological nature but also astrophysical, such as binary systems or neutron stars, that can be found all across our galaxy and the visible Universe in general. The main reason/excuse for this "failure" is the weakness of the gravitational interaction, translated of course as the smallness of the gravitational Newton's constant G_N which can be found as a factor in the Einstein's equation. Thus even a seemingly strong source will emit a very small amount of gravitational radiation. The extraordinary sensitivity of equipment needed in order to detect such a tiny ripple of spacetime is a real challenge to the current technology with the examples of LIGO and LISA as its best representatives.

In section 2 we will review the basic calculations and results of the theory of gravitational waves, and will introduce the notions and quantities that will be necessary for understanding how GW's are produced in the early Universe and how they evolve from then to now. In section 3 we will specifically deal with GW's of cosmological origin and several production mechanisms. We will give a qualitative estimate of the spectrum of the expected stochastic background and distinguish between different cosmological scenarios. The indirect experimental restrictions on the amplitude of the GW spectra will

be explained in section 4, and finally, the current experimental progress for GW detection and future expectations will be overviewed in section 5, along with some facts and figures for the updated LIGO and the well anticipated LISA detectors.

2 Basic Theory of Gravitational Waves

Reformulating GR in terms of perturbations around exact solutions will lead us to a linearized version of the Einstein equations

$$R_{\mu\nu} - \frac{1}{2} g_{\mu\nu} R = 8\pi G_N. \tag{1}$$

The notion of gravitational waves will be defined by means of these metric perturbations, as it will be shown that they comprise propagating field modes that travel at the speed of light.

2.1 Perturbing flat spacetime

The mathematical formulation of General Relativity as a geometrical theory of gravitation consists of a set of 10 highly non-linear 2nd order differential equations. Such a dynamical system is usually impossible to solve analytically in a generic manner. There are certain very special geometries and matter distributions that provide us with a handful of very interesting, exact analytical solutions for the Einstein's equation. However, these configurations usually exhibit an unnaturally high degree of symmetry, which of course only belongs to the idealized world of mathematics and cannot be found in nature.

What is actually found in nature can be sometimes extremely close to these special solutions and their use as good approximations to physical systems is what makes them so important. For instance, the geometry of spacetime around a star can be approximated to very good accuracy by the Schwartzschild metric, even though in reality a star can never be perfectly spherically symmetric.

For this reason it is useful to study small metric perturbations around such configurations, which we can consider as *background metric* configurations and denote as $\bar{g}_{\mu\nu}$. By the word *small* it is actually implied that the entries of the actual tensor components $g_{\mu\nu}$ are very close to the unperturbed values of $\bar{g}$.

To make this more mathematically concise, let $(M, g_{\mu\nu})$ be the actual spacetime that naturally satisfies the Einstein equation. Then we call it

a perturbation around a background spacetime $(M, \bar{g}_{\mu\nu})$ if we can globally define a tensor $h_{\mu\nu}$ such that

$$g_{\mu\nu} = \bar{g}_{\mu\nu} + h_{\mu\nu} \quad , \quad |h_{\mu\nu}| \ll 1 \tag{2}$$

The most common exact solution and the most trivial one that one can think of is of course the Minkowski metric $\eta_{\mu\nu}$ which corresponds to an empty flat spacetime. Of course this is not exactly what we are looking for as a global solution in a realistic cosmological theory, since it restricts all of spacetime to be free from any kind of strong matter distribution.

However it is quite instructive to begin our calculations for the specific simple case of a flat Minkowski background spacetime and then examine the more generic perturbation theory around an arbitrary background. This way we can get a first insight on what a gravitational wave really is and how it locally behaves when propagating in (almost) empty space. So let us begin with just

$$g_{\mu\nu} = \eta_{\mu\nu} + h_{\mu\nu} \quad , \quad |h_{\mu\nu}| \ll 1 \quad , \quad \eta_{\mu\nu} = diag(-1, 1, 1, 1), \tag{3}$$

where we used natural units $c = 1$ as will be the case in all of our calculations. This is the so-called *weak field approximation.*

2.2 Linearizing everything

Now we can rewrite all important quantities of GR in terms of this expansion and find some nontrivial properties, in contrast to just flat spacetime. Even better, we can restrict to a linearized version of them, keeping only terms up to linear order in $h_{\mu\nu}$. The Christoffel connection now reads :

$$\begin{aligned} \Gamma^{\lambda}_{\mu\nu} &= \frac{1}{2}(\eta^{\lambda\rho} + h^{\lambda\rho})[\partial_\mu h_{\nu\rho} + \partial_\nu h_{\mu\rho} - \partial_\rho h_{\mu\nu}] \\ &= \frac{1}{2}\eta^{\lambda\rho}(\partial_\mu h_{\nu\rho} + \partial_\nu h_{\mu\rho} - \partial_\rho h_{\mu\nu}) + O(h^2) \end{aligned} \tag{4}$$

The linearized Riemann and Ricci tensors will be free of the $\Gamma\Gamma$ terms since each Γ is purely 1st order in h. More explicitly :

$$\begin{aligned} R^{(1)}_{\mu\nu} &= \partial_\lambda \Gamma^{\lambda}_{\mu\nu} - \partial_\mu \Gamma^{\lambda}_{\lambda\nu} \\ &= \frac{1}{2}\eta^{\lambda\rho}\left[\partial_\lambda\partial_\mu h_{\nu\rho} + \partial_\lambda\partial_\nu h_{\mu\rho} - \partial_\lambda\partial_\rho h_{\mu\nu} - \partial_\mu\partial_\lambda h_{\nu\rho} - \partial_\mu\partial_\nu h_{\lambda\rho} + \partial_\mu\partial_\rho h_{\nu\lambda}\right] \\ &= \frac{1}{2}\left[-\Box h_{\mu\nu} - \partial_\mu\partial_\nu h + 2\partial_{(\mu}\partial^{\lambda}h_{\nu)\lambda}\right] \end{aligned} \tag{5}$$

and the Ricci scalar,

$$R^{(1)} = \eta^{\mu\nu} R^{(1)}_{\mu\nu} = \partial^\mu \partial^\lambda h_{\mu\lambda} - \Box h \quad , \tag{6}$$

where we denote $\Box = \partial_\mu \partial^\mu = \partial_t^2 - \nabla^2$ as the d'Alembertian, and h is just the trace h^μ_μ.

So now we can write down the linearized Einstein tensor.

$$\begin{aligned} G^{(1)}_{\mu\nu} &= R^{(1)}_{\mu\nu} - \frac{1}{2}\eta_{\mu\nu} R^{(1)} \\ &= \frac{1}{2}(-\Box h_{\mu\nu} - \partial_\mu \partial_\nu h + 2\partial^\rho \partial_{(\mu} h_{\nu)\rho} - \eta_{\mu\nu}\partial^\rho \partial^\lambda h_{\rho\lambda} + \eta_{\mu\nu}\Box h) \end{aligned} \tag{7}$$

From the field theoretical point of view, the absence of higher order terms implies a non-interacting classical field theory for the tensor field of perturbations. So by linearizing the Einstein equation we actually have formulated a free tensor field theory, or, in terms of representations of the Lorentz group, a free spin-2 field theory which we will later identify with the graviton.

To simplify the above expression for the Einstein tensor it will prove convenient to first introduce the *trace reversed* metric perturbation $\bar{h}_{\mu\nu} = h_{\mu\nu} - \frac{1}{2}\eta_{\mu\nu} h$ [1] , the name coming obviously from $\bar{h} = h - \frac{1}{2}4h = -h$. Re-expressing $G_{\mu\nu}$ in terms of $\bar{h}$ will give :

$$\begin{aligned} G^{(1)}_{\mu\nu} =& \frac{1}{2}\Big[-\Box \bar{h}_{\mu\nu} + \frac{1}{2}\eta_{\mu\nu}\Box \bar{h} + \partial_\mu \partial_\nu \bar{h} + 2\partial^\rho \partial_{(\mu} \bar{h}_{\nu)\rho} - \partial_\mu \partial_\nu \bar{h} - \eta_{\mu\nu}\partial^\rho \partial^\lambda \bar{h}_{\rho\lambda} \\ &+ \frac{1}{2}\eta_{\mu\nu}\Box \bar{h} - \eta_{\mu\nu}\Box \bar{h}\Big] \\ =& -\frac{1}{2}\Box \bar{h}_{\mu\nu} + \partial^\rho \partial_{(\mu} \bar{h}_{\nu)\rho} - \frac{1}{2}\eta_{\mu\nu}\partial^\rho \partial^\lambda \bar{h}_{\rho\lambda} \end{aligned} \tag{8}$$

2.3 Gauge transformations

Now if we remember the gauge freedom of GR which is of course the fundamental property of *diffeomorphism invariance* implied by the equivalence principle, we can further simplify our calculations. Different metric configurations that correspond to the same class, by means of being equivalent up to diffeomorphisms, describe the same physical spacetime. This means that starting from a metric perturbation $h_{\mu\nu}$ we can reach any metric $h'_{\mu\nu}$ in its

[1] Another way to get rid of 2 terms which was used in earlier literature, including [1], would be to contract (1) and find $R = -8\pi G_N T$, then replacing the source with $S_{\mu\nu} = T_{\mu\nu} - \frac{1}{2}\eta_{\mu\nu} T$ leaving only the 4 terms of $R_{\mu\nu}$ on the LHS.

equivalence class by performing the appropriate smooth coordinate transformation : $x^\mu \to x'^{\bar{\mu}} + \xi^\mu(x)$. Let us consider the infinitesimal transformations which will generate diffeomorphisms by changing the vector field ξ^μ above with a weakly varying ϵ^μ, where $\partial_\nu \epsilon^\mu$ is of the order of $h_{\mu\nu}$, and see how the metric perturbation is transformed.

$$g'^{\bar{\mu}\bar{\nu}} = \frac{\partial x^{\bar{\mu}}}{\partial x^\mu}\frac{\partial x^{\bar{\nu}}}{\partial x^\nu} g^{\mu\nu} \quad , \quad \frac{\partial x^{\bar{\mu}}}{\partial x^\mu} = \left(\delta^{\bar{\mu}}_\mu + \frac{\partial \epsilon^{\bar{\mu}}}{\partial x^\mu}\right)$$

$$g'^{\bar{\mu}\bar{\nu}} = \left(\delta^{\bar{\mu}}_\mu \delta^{\bar{\nu}}_\nu + \delta^{\bar{\mu}}_\mu \frac{\partial \epsilon^{\bar{\nu}}}{\partial x^\nu} + \delta^{\bar{\nu}}_\nu \frac{\partial \epsilon^{\bar{\mu}}}{\partial x^\mu}\right) g^{\mu\nu} + O(\partial\epsilon^2) \tag{9}$$

Now to linear order in $h_{\mu\nu}$, the reverse metric is $g^{\mu\nu} = \eta^{\mu\nu} - h^{\mu\nu}$:

$$g^{\mu\nu} g_{\nu\lambda} = \eta^\mu \eta_{\nu\lambda} + \overbrace{\eta^{\mu\nu} h_{\nu\lambda} - h^{\mu\nu}\eta_{\nu\lambda}}^{\approx h^\mu_\lambda - h^\mu_\lambda = 0} + O(h^2) \approx \delta^\mu_\lambda$$

So we have

$$\begin{aligned} g'^{\bar{\mu}\bar{\nu}} &= \eta^{\bar{\mu}\bar{\nu}} - h^{\bar{\mu}\bar{\nu}} + \eta^{\bar{\mu}\nu}\partial_\nu \epsilon^{\bar{\nu}} + \eta^{\mu\bar{\nu}}\partial_\mu \epsilon^{\bar{\mu}} + O(h^2) \\ \Rightarrow \eta^{\bar{\mu}\bar{\nu}} - h'^{\bar{\mu}\bar{\nu}} &= \eta^{\bar{\mu}\bar{\nu}} - h^{\bar{\mu}\bar{\nu}} + \partial_\nu \epsilon^{\bar{\nu}} \eta^{\bar{\mu}\nu} + \eta^{\mu\bar{\nu}}\partial_\mu \epsilon^{\bar{\mu}} \\ \Rightarrow h'^{\mu\nu} &= h^{\mu\nu} - \eta^{\mu\lambda}\partial_\lambda \epsilon^\nu - \eta^{\lambda\nu}\partial_\mu \epsilon^\mu \end{aligned}$$

and finally

$$h'_{\mu\nu} = h_{\mu\nu} - \partial_\mu \epsilon_\nu - \partial_\nu \epsilon_\mu \quad . \tag{10}$$

2.4 Fixing the gauge

Now that we know how $h_{\mu\nu}$ transforms under gauge transformations we can use this to cast the Einstein equation in a simpler and more useful form. One can easily show that every diffeomorphism class of metrics has a metric that satisfies the *de Donder gauge* condition $\partial^\mu \bar{h}_{\mu\nu} = 0$, which can be interpreted as a condition of transversality. Starting from a generic metric of a non-vanishing divergence (non-Lorenz) we can find a field ϵ_μ such that the new metric $h'_{\mu\nu}$ does satisfy the Lorenz gauge condition. In order to get there we can see that $h' = h - 2\partial_\mu \epsilon^\mu$ and

$$\begin{aligned} \bar{h}'_{\mu\nu} &= h'_{\mu\nu} - \frac{1}{2}\eta_{\mu\nu} h' = h_{\mu\nu} - \partial_\mu \epsilon_\nu - \partial_\nu \epsilon_\mu - \frac{1}{2}\eta_{\mu\nu} h + \eta_{\mu\nu}\partial_\rho \epsilon^\rho \\ &= \bar{h}_{\mu\nu} - 2\partial_{(\mu}\epsilon_{\nu)} + \eta_{\mu\nu}\partial_\rho \epsilon^\rho \end{aligned} \tag{11}$$

so if we want h' to be in the Lorenz gauge, we need $\partial^\mu \bar{h}'_{\mu\nu}$ to vanish. On the other hand

$$\partial^\mu \bar{h}'_{\mu\nu} = \partial^\mu \bar{h}_{\mu\nu} - \Box \epsilon_\nu - \partial^\mu \partial_\nu \epsilon_\mu + \partial_\nu \partial^\rho \epsilon_\rho = \partial^\mu \bar{h}_{\mu\nu} - \Box \epsilon_\nu \tag{12}$$

so we require a coordinate transformation, where $\Box\epsilon_\nu = \partial^\mu h_{\mu\nu}$. This results in a first-order differential equation that always has a solution for the field $\epsilon_\mu(x)$.

Under the choice of gauge described above, we rewrite the simplified Einstein's equation which now reads

$$\Box\bar{h}_{\mu\nu} = -16\pi G_N T_{\mu\nu} \quad . \tag{13}$$

From the nature of the differential equation the wave-like propagation of a metric perturbation is manifest, as well as the fact that a free gravitational wave will propagate at the speed of light. If one is only interested in studying the propagation of gravitational waves in vacuum, then one can eliminate the source term which gives the homogeneous "box" equation

$$\Box\bar{h}_{\mu\nu} = 0 \quad . \tag{14}$$

At this point we can further fix the gauge having the freedom to add terms corresponding to transformations of $\Box\epsilon_\mu = 0$. The trace reversed metric now transforms as

$$\bar{h}'_{\mu\nu} = \bar{h}_{\mu\nu} + \eta_{\mu\nu}\partial^\rho\epsilon_\rho - \partial_\mu\epsilon_\nu - \partial_\nu\epsilon_\mu \tag{15}$$

to a metric that also satisfies the Lorenz gauge and equation of motion (14). We can carefully choose this gauge to eliminate 4 more independent components of the metric perturbation tensor leaving us with $10 - 4 - 4 = 2$ independent *physical* degrees of freedom that actually correspond to the 2 polarizations of the gravitational wave. The choice is made in such a way that the trace vanishes $\bar{h} = 0 = h$ (thus $\bar{h}_{\mu\nu} = h_{\mu\nu}$), as well as the longitudinal components $h^{0i} = h^{i0} = 0$. This will finally result to the (spatial) metric perturbation in the *transverse traceless* gauge h^{TT}_{ij} where only two transverse tensorial modes survive, corresponding to planes normal to the vector of propagation. If we identify the z-axis as the direction of propagation, then the metric perturbation will be written in the familiar form

$$h^{TT}_{\mu\nu} = \begin{pmatrix} 0 & 0 & 0 & 0 \\ 0 & h_+ & h_\times & 0 \\ 0 & h_\times & -h_+ & 0 \\ 0 & 0 & 0 & 0 \end{pmatrix} f(\omega t - z) \quad . \tag{16}$$

In fact, from now on we will only keep the spatial indices notation h^{TT}_{ij} since in the TT gauge, all 0μ components vanish. We can also define the projection operator $P_{ij}(\hat{\mathbf{k}}) = \delta_{ij} - n_i n_j$, which, given a unit vector $\hat{\mathbf{k}}$, projects any given tensor to the plane normal to it. In order to project on the TT part we also have to eliminate the trace, which will result in

$$\Pi_{ij,lm}(\hat{\mathbf{k}}) = P_{il}(\hat{\mathbf{k}})P_{jm} - \frac{1}{2}P_{ij}(\hat{\mathbf{k}})P_{lm}(\hat{\mathbf{k}}) \tag{17}$$

Contracting this operator with any given spatial tensor S_{ij} will give the TT part of it, S_{ij}^{TT}.

2.5 Adding the sources

The next step would be to put the source term $T_{\mu\nu}$ back in the RHS and try to solve the wave equation (13) for a generic nonvanishing source. This can be done via the Green's function of the d'Alembertian which is well known

$$\Box G(x;x') = \delta^{(4)}(x-x') \quad \Rightarrow \quad G(x;x') = -\frac{\delta\left(t' - \left[t - \frac{|\vec{x}-\vec{x}'|}{c}\right]\right)}{4\pi|\vec{x}-\vec{x}'|} \tag{18}$$

and now the general solution of (13) will be

$$\bar{h}_{\mu\nu}(t,\vec{x}) = 4G_N \int d^3\vec{x}' \frac{T_{\mu\nu}(t-|\vec{x}-\vec{x}'|,\vec{x}')}{|\vec{x}-\vec{x}'|} \tag{19}$$

Now one needs to keep in mind that one cannot go to the TT gauge, since there is no residual gauge as in the homogeneous case. However it can be shown that we can still decouple the TT *part* of the metric, which will be sourced by the TT part of the stress-energy tensor. The remaining gravitational degrees of freedom do not actually propagate, but only satisfy Poisson-like equations.

2.6 The quadrupole formula

We now place ourselves as observers far away from the non-vacuum distribution of mass-energy density, which we suppose that is concentrated within a small region outside which it vanishes. The main assumption that we make is that we consider the characteristic size of the source L to be much smaller than our distance from the distribution r (which is usually the case for astrophysical observations). Under the above condition we can approximate the distance from the integrated region $|\vec{x}-\vec{x}'|$ to be in first order equal to r. More analytically:

$$|\vec{x}-\vec{x}'| = \sqrt{\vec{x}^2 + \vec{x}'^2 - 2x_i x'^i} \approx |\vec{x}| = r \quad , \tag{20}$$

where $|\vec{x}'| \leq L \ll r$.

Now the integral (19) becomes

$$\bar{h}_{\mu\nu} = \frac{4G_N}{r} \int d^3\vec{x}' T_{\mu\nu}(t-r,\vec{x}') \tag{21}$$

In the end we are interested in the TT part only, so we consider the spatial part $T_{ij}(t-r,\vec{x}')$ which we will focus on, in order to get a nicer expression for h_{ij}. Remember that we are working up to first order around a flat background, so the *Bianchi identities* for $T_{\mu\nu}$ yield $\partial^\mu T_{\mu\nu}=0$ therefore

$$\partial^0 T_{0i}+\partial^j T_{ij}=0\Rightarrow\partial^j T_{ij}=-\partial^0 T_{0i} \tag{22}$$

$$\partial^0 T_{00}+\partial^i T_{0i}=0\Rightarrow\left(\partial^0\right)^2 T_{00}\partial^i\partial^0 T_{0i}=0 \tag{23}$$

$$\Rightarrow\left(\partial^0\right)^2 T_{00}=\partial^k\partial^l T_{kl} \tag{24}$$

and if we multiply by $x^i x^j$ we will eventually get

$$\frac{\partial^2}{\partial t^2}(T_{00}x^i x^j)=\partial_k\partial_l(T^{kl}x^i x^j)-2\partial_k\left[x^i T^{kj}+x^j T^{ki}\right]+2T^{ij} \tag{25}$$

Now replacing T^{ij} in (21) we conclude

$$\begin{aligned}\bar{h}_{ij}&=\frac{4G_N}{r}\int d^3\vec{x}'\frac{1}{2}\frac{\partial^2}{\partial t^2}\left[T_{00}(t-r,\vec{x}')x'^i x'^j\right]+b.t.\\&=\frac{2G_N}{r}\frac{\partial^2}{\partial t^2}\int d^3\vec{x}'\left[\rho(t-r,\vec{x}')x'^i x'^j\right]\end{aligned} \tag{26}$$

This is the famous quadrupole formula, which identifies the quadrupolar moment of the energy (or usually mass) distribution of the source as the generator of metric perturbations, while these propagate according to a $1/r$ law. Now it is easy to go to the TT part in order to get the physical propagating degrees of freedom, leaving us with the final result

$$h_{ij}^{TT}(t,\vec{x})=\frac{2G_N}{r}\Pi_{ij,lm}(\hat{\mathbf{x}})\frac{\partial^2}{\partial t^2}\int d^3\vec{x}'\left[\rho(t-r,\vec{x}')x'^l x'^m\right] \tag{27}$$

2.7 Perturbations around a generic background

Now we can try to extend our calculations to the more interesting general case of a non-Minkowskian background. Let $\bar{g}_{\mu\nu}$ be the background spacetime metric around which small perturbations are considered and denoted by $h_{\mu\nu}$. So now the real spacetime metric will be

$$g_{\mu\nu}=\bar{g}_{\mu\nu}+h_{\mu\nu}. \tag{28}$$

Usually, and for the purpose of this project $\bar{g}_{\mu\nu}$ is just the FLRW spacetime metric, namely $\mathrm{diag}[-1,a^2,a^2,a^2]$, $a=a(t)$. We will also denote all quantities related to the background spacetime metric by barring over, and use $\bar{g}$ to raise and lower indices.

We again start from the Christoffel symbols:

$$\begin{aligned}\Gamma^{\lambda}_{\mu\nu} =&\frac{1}{2}\left[\bar{g}^{\lambda\rho} - h^{\lambda\rho}\right]\left[\partial_\mu \bar{g}_{\rho\nu} + \partial_\mu h_{\rho\nu} + \partial_\nu \bar{g}_{\rho\mu} + \partial_\nu h_{\rho\nu} - \partial_\rho \bar{g}_{\mu\nu} - \partial_\rho h_{\mu\nu}\right]\\ =&\frac{1}{2}\bar{g}^{\lambda\rho}\left(\partial_\mu \bar{g}_{\rho\nu} + \partial_\nu \bar{g}_{\rho\mu} - \partial_\rho \bar{g}_{\mu\nu}\right) + \frac{1}{2}\bar{g}^{\lambda\rho}\left(\partial_\mu h_{\rho\nu} + \partial_\nu h_{\rho\mu} - \partial_\rho h_{\mu\nu}\right)\\ &- \frac{1}{2}h^{\lambda\rho}\left(\partial_\mu \bar{g}_{\rho\nu} + \partial_\nu \bar{g}_{\rho\mu} - \partial_\rho \bar{g}_{\mu\nu}\right) + O(h^2)\\ =&\bar{\Gamma}^{\lambda}_{\mu\nu} - h^{\lambda\kappa}\bar{g}_{\kappa\sigma}\bar{\Gamma}^{\sigma}_{\mu\nu} + \frac{1}{2}\bar{g}^{\lambda\rho}\left(\partial_\mu h_{\rho\nu} + \partial_\nu h_{\rho\mu} - \partial_\rho h_{\mu\nu}\right),\end{aligned} \tag{29}$$

where we have used in the last step $h^{\lambda\rho} = h^{\lambda\sigma}\delta^{\rho}_{\sigma}$. We can rewrite this in a covariant form if we notice from the definition of the covariant derivative on a (0,2) tensor field:

$$\begin{aligned}\partial_\mu h_{\rho\nu} &= \bar{\nabla}_\mu h_{\rho\nu} + \bar{\Gamma}^{\lambda}_{\mu\rho}h_{\lambda\nu} + \bar{\Gamma}^{\lambda}_{\mu\nu}h_{\lambda\rho}\\ \partial_\nu h_{\rho\mu} &= \bar{\nabla}_\nu h_{\rho\mu} + \bar{\Gamma}^{\lambda}_{\nu\rho}h_{\lambda\mu} + \bar{\Gamma}^{\lambda}_{\nu\mu}h_{\lambda\rho}\\ \partial_\rho h_{\mu\nu} &= \bar{\nabla}_\rho h_{\mu\nu} + \bar{\Gamma}^{\lambda}_{\rho\mu}h_{\lambda\nu} + \bar{\Gamma}^{\lambda}_{\rho\nu}h_{\lambda\mu}\end{aligned}$$

and subtract the 3rd relation from the sum of the other two.

$$\Rightarrow \Gamma^{\lambda}_{\mu\nu} = \bar{\Gamma}^{\lambda}_{\mu\nu} + \delta\Gamma^{\lambda}_{\mu\nu}, \tag{30}$$

where we define the connection perturbation

$$\delta\Gamma^{\lambda}_{\mu\nu} = \frac{1}{2}\bar{g}^{\lambda\rho}\left(\nabla_\mu h_{\rho\nu} + \nabla_\nu h_{\rho\mu} - \nabla_\rho h_{\mu\nu}\right) \tag{31}$$

We can now continue with the Riemann curvature and Ricci tensor up to 1st order in h and thus in $\delta\Gamma$

$$\begin{aligned}R^{\rho}_{\sigma\mu\nu} = \partial_\mu\bar{\Gamma}^{\rho}_{\sigma\nu} - \partial_\nu\bar{\Gamma}^{\rho}_{\sigma\mu} + \partial_\mu\delta\Gamma^{\rho}_{\sigma\nu} - \partial_\nu\delta\Gamma^{\rho}_{\sigma\mu}&\\ = \bar{R}^{\rho}_{\sigma\mu\nu} + \delta R^{\rho}_{\sigma\mu\nu}&\end{aligned} \tag{32}$$

where again a covariant form can be obtained for the curvature perturbation, which will hold for all coordinate systems:

$$\delta R^{\rho}_{\sigma\mu\nu} = \bar{\nabla}_\mu\delta\Gamma^{\rho}_{\sigma\nu} - \bar{\nabla}_\nu\delta\Gamma^{\rho}_{\sigma\mu} \tag{33}$$

The Ricci tensor reads

$$\begin{aligned}\delta R_{\sigma\nu} =&\delta R^{\rho}_{\sigma\rho\nu} = \bar{\nabla}_\rho\delta\Gamma^{\rho}_{\sigma\nu} - \bar{\nabla}_\nu\delta\Gamma^{\rho}_{\sigma\rho}\\ =&\frac{1}{2}\left[\bar{\nabla}_\rho\bar{\nabla}_\sigma h^{\rho}_{\nu} + \bar{\nabla}_\rho\bar{\nabla}_\nu h^{\rho}_{\sigma} - \bar{\Box}h_{\sigma\nu} - \bar{\nabla}_\nu\bar{\nabla}_\sigma h - \bar{\nabla}_\nu\bar{\nabla}_\rho h^{\rho}_{\sigma} + \bar{\nabla}_\nu\bar{\nabla}_\rho h^{\rho}_{\sigma}\right]\\ =&-\frac{1}{2}\bar{\Box}h_{\sigma\nu} - \frac{1}{2}\bar{\nabla}_\nu\bar{\nabla}_\sigma h + \bar{\nabla}_\rho\bar{\nabla}_{(\sigma}h^{\rho}_{\nu)} \quad ,\end{aligned} \tag{34}$$

where the barred d'Alambertian stands for $\bar{\Box} = \bar{g}^{\mu\nu}\bar{\nabla}_\mu\bar{\nabla}_\nu$.

The Einstein equation will be too long to keep track of so we go back to the trace-reversed metric $\bar{h}_{\mu\nu}$ as defined before (8) (the bar here having nothing to do of course with the background). The Ricci scalar perturbation will simply be

$$\delta R = \bar{g}^{\mu\nu}\delta R_{\mu\nu} - h^{\mu\nu}\bar{R}_{\mu\nu} \tag{35}$$

and finally putting everything together in the trace reversed description we get the Einstein tensor perturbations

$$\begin{aligned}\delta G_{\mu\nu} = 0 &= \delta R_{\mu\nu} + R_{\rho\nu\mu\sigma}h^{\rho\sigma} \\ &= -\frac{1}{2}\bar{\Box}\bar{h}_{\mu\nu} + \frac{1}{4}\bar{g}_{\mu\nu}\bar{\Box}\bar{h} + \bar{\nabla}_\rho\bar{\nabla}_{(\sigma}\bar{h}^\rho_{\nu)} + \frac{1}{2}\bar{\nabla}_{[\nu}\bar{\nabla}_{\sigma]}\bar{h} + R_{\rho\nu\mu\sigma}h^{\rho\sigma}\end{aligned} \tag{36}$$

We can further simplify the above expression by choosing an appropriate gauge transformation by means of a vector field whose box is equal to $\bar{\nabla}^\mu\bar{h}_{\mu\nu}$ so that we end up with a divergence-free metric perturbation $\bar{h}'_{\mu\nu}$. To keep a long story short, following the same arguments as in the flat background case, and carefully using arguments of general covariance, we conclude with the linearized Einstein equation in the TT gauge (we will drop the TT index notation)

$$\delta G_{\mu\nu} = -\frac{1}{2}\bar{\Box}h_{\mu\nu} + \bar{R}_{\rho\nu\mu\sigma}h^{\rho\sigma} \quad . \tag{37}$$

Gravitational waves (GWs) can still be well defined in such a spacetime in the sense of the so called *geometric optics regime* [2], where the wavelength of the perturbation is much smaller than the characteristic scale in which the average metric changes significantly. GWs can also be considered as rapidly varying perturbations over a relatively static background.

2.8 Effective GW energy

The last missing piece, which we will need for the following sections comes from the extension of the former discussion to second order perturbations. Roughly speaking, consider a stress energy tensor which is constructed so that the Einstein equation is satisfied exactly if one puts the background Einstein tensor on the LHS. This can be viewed as the Einstein equation in zeroth order of perturbation. If we subtract this tensor from the actual stress-energy tensor, then what is left is defined as the effective stress-energy tensor of the gravitational wave. It turns out that the first order terms vanish by virtue of the linearized Einstein equation and only 2nd order perturbative terms survive.

I will only summarize the results for the effective stress-energy tensor in the covariantly transverse traceless gauge, which is given by the rather simple expression

$$t^{gw}_{\mu\nu} = \frac{1}{32\pi G_N}\bar{\nabla}_\mu h_{\lambda\rho}\bar{\nabla}_\nu h^{\lambda\rho}. \tag{38}$$

In principle we will only need the 00 component of it, namely the effective energy density of the gravitational wave.

3 Cosmological Stochastic Backgrounds

During the last few decades, a great deal of research has been made towards the study of Astrophysical and Cosmological sources of gravity waves. The above distinction is referring to the origin of the radiation and the scale of its production process. The most important types of astrophysical sources are (i) coalescing binary star systems composed of neutron stars and/or black holes, (ii) pulsars and (iii) certain kinds of supernovae.

Because of the large scale of the Planck mass $M_{Pl} \sim 10^{19} GeV$, which defines the gravitational coupling constant ($G_N = \hbar c/M^2_{Pl}$), gravitons decoupled very early in the evolution of the Universe and freely streamed up to the present day, totally undisturbed by even the most dense matter distributions that we know of today. We are expecting a *background* of "cosmic" gravitational radiation to emerge from the early stages of the Universe, when a series of large scale phenomena is believed to have taken place, leading to intense gravitational wave production. This type of background is characterized as *stochastic*, since it consists of a great number of *unresolved* sources randomly distributed throughout the entire Universe. Under the assumption that the Universe is *homogeneous* and *isotropic* on relatively large scales, this background is expected to be rather isotropic as well. However a stochastic background of gravitational waves sourced by a large number of *astrophysical* unresolved sources is also predicted. These sources for example may correspond to the abundance of binary star systems, plenty of which populate our own Milky Way, and, given the angular resolutions of the close future GW detectors, they cannot be distinguished from one-another. As a consequence of the small scale anisotropy, the astrophysical stochastic background will not be isotropic, being more intense for angles that correspond to the plane of our galactic disc.

From now on we are only interested in Cosmological GW's, coming from the primordial Universe. The recent progress made towards a successful cosmological model and the variety of inflationary scenarios that emerged from this effort provide us with a number of mechanisms for gravity wave

production during the early stages of the Universe. The most important of these processes (some of which will be discussed here) are

- fluctuation amplification during inflation
- preheating and inflaton decay
- cosmic strings
- 1st order phase transitions
- pre-big-bang scenarios
- branes, quintessence, magnetic fields, turbulence etc.

The spectrum of each mechanisms covers a wide range of frequencies and scales quite uniquely. The lowest possible frequency will correspond to the largest wavelength of oscillation, which is of course bounded by the (causal) scale of the Universe, so of the order of Hubble length. This amounts to $\lambda \leq H_0^{-1}$ giving a lowest frequency today of $f \geq 10^{-18} Hz$. On the other hand, the highest frequency waves correspond to the highest temperature of the primordial Universe, which is taken to be the Planck scale $T \approx 10^{32} K$, since gravitons do not freely stream above this temperature and quantum gravity effects become important. This highest end of the frequency band today is of the order of $10^{12} Hz$, taking into account the redshift in an FLRW Universe.

For the moment, present day and near future detectors cover the range of 7 orders of magnitude, between $0.1 mHz$ (LISA) and kHz (ground based interferometers). Given the sensitivity that is predicted to be reached, most of the spectra of the above processes are not likely to be strong enough for detection.

3.1 Preliminaries

The Cosmological stochastic background can be viewed as a (usually isotropic and unpolarized) superposition of gravity waves of all frequencies coming from all angles which is expressed by the expansion

$$h_{ij}(t, \vec{x}) = \sum_{P=+,\times} \int_{-\infty}^{+\infty} df \int d\hat{k} h_P(f, \hat{k}) e^{-2\pi i f t} \epsilon_{ij}^P(\hat{k}) e^{i\vec{k}\cdot\vec{x}} + c.c. \qquad (39)$$

so all the important information are held in $h_P(f, \hat{k})$ or equivalently, in the unpolarized and isotropic case, just h_k (in terms of the wavenumber $k = 2\pi f$),

defined by

$$h_{ij}(t,\vec{x}) = \int \frac{d^3\vec{k}}{(2\pi)^{3/2}} h_k(t) e^{i\vec{k}\vec{x}} \sum_P \epsilon_{ij}^P(\hat{k}) + c.c. \quad , \tag{40}$$

which will provide us with the *spectrum* of the gravitational background. Here $\hat{k}$ denotes the incoming unit vector of propagation, $d\hat{k} = d\phi d\cos\theta$, and $\epsilon_{ij}^P(\hat{k})$ is just the polarization tensor for plus or cross polarization normal to $\hat{k}$

It would be useful if we could express the results for a certain spectrum in terms of a familiar quantity in cosmology, the gravitational wave *energy density* spectrum Ω_{gw} [2] defined as the differential density of effective energy over logarithmic frequency bins measured in units of critical density:

$$\Omega_{gw}(f) = \frac{1}{\rho_c}\frac{d\rho_{gw}}{d\log f} = \frac{1}{\rho_c} f \frac{d\rho_{gw}}{df} \tag{41}$$

Now we just need to relate ρ_{gw} to the Fourier transformed h_k, which is done using the effective GW energy formula (38)

$$\rho_{gw} = t_{00} = \frac{1}{32\pi G_N} \left\langle \dot{h}_{ij} \dot{h}^{ij} \right\rangle \tag{42}$$

when the averaging takes place over several wavelengths. However, in a stochastic background, this is equivalent with taking the *ensemble average*.

The bottom line is that today's Universe abundance in gravitons of any given energy can be directly calculated and translated in terms of Ω_{gw}, if we can somehow track down the evolution of the metric perturbations h_k back to their sources, even when we can only describe them as random (stochastic) configurations. This can be studied for each scenario individually.

It is also useful to come up with some general rules that dictate how the spectrum has evolved within the FLRW Universe, from a given time, when we suppose that the sources vanish, until the present day. The important quantity here is the scale factor a, whose scaling with time depends on the equation of state $w = \frac{p}{\rho}$ according to $a \propto t^{2/(3+3w)}$. For a radiation dominated Universe $w = 1/3$. The amplitude scales as $\Omega_{gw} \propto a^{-4}$ as shown in (59)

[2] However, the quantity $\rho_c = \frac{3H_0^2}{8\pi G_N}$ is by definition determined by the value of the Hubble parameter today and thus carries with it a certain error, expressed as an uncertainty of H_0's measurement, h defined by $H_0 = 100h$ km/s/Mpc. Today's evaluation for the value of h is $h_0 = 0.72 \pm 0.02$ and it changes as new observations are considered (e.g. WMAP). For this reason all theoretical predictions and experimental results are expressed in terms of the error-independent $h_0^2\Omega_{gw}$.

below. The temperature on the other hand does not have a direct scaling rule for the scale factor a but a rather more complicated dependence, which involves a few statistical assumptions. However, supposing that chemical equilibrium was always satisfied for a specific time interval in the history of the Universe, then the entropy per unit volume is conserved and the scaling goes like

$$g_{*s}T_*^3 a_*^3 = g_{0s}T_0^3 a_0^3 \tag{43}$$

where g_s is the number of effective relativistic degrees of freedom for the entropy and for the processes of interest in the very early Universe, $g_{*s} = 106.75$ at least. This implies that at temperature scales as high as $T > 100GeV$, all Standard Model particles are relativistic.

As a naive result, which is based on the false assumption that equilibrium was preserved since the gravitons decoupled, todays black body temperature for the relic graviton bath, can be estimated to be $\sim 0.9K$ given the current temperature of the photon fluid $2.73K$. This follows from

$$T_{gr} = \left[\frac{g_{0s}}{g_{*S}}\right]^{1/3} T_0, \tag{44}$$

which is a consequence of (43)

3.2 Amplification of Quantum Fluctuations

A general mechanism that is activated during the inflationary epoch is the amplification of initial quantum fluctuations of fields and was first discovered and studied by Grishchuk and Starobinsky in the mid 70's. The basic concept behind this process is that, assuming a quantum gravity epoch above the Planck scale, the very early Universe inherited quantum fluctuations, and fields would deviate from absolute homogeneity. As the Universe expanded dramatically during inflation, some of these fluctuations were amplified as shown below. After the end of inflation, the amplified tensor perturbations continued as propagating gravity waves, undergoing the usual cosmological redshift as $\vec{k}_{phys}(t) = \vec{k}\frac{a(0)}{a(t)}$, where $a(t)$ is the scale factor.

We will now consider a standard FLRW cosmological model(even though this requires large scale homogeneity), where the metric will have the form $\bar{g}_{\mu\nu} = diag[-1, a^2(t), a^2(t), a^2(t)]$ and continue with an explicit calculation for equation (37). It can be shown [3] that it simplifies to the homogeneous scalar d'Alembertian equation :

$$\bar{\Box}_S h_i{}^j(t, \vec{x}) = \frac{1}{\sqrt{-\bar{g}}}\partial_\mu \sqrt{-\bar{g}}\bar{g}^{\mu\nu}\partial_\nu h_i{}^j = 0 \tag{45}$$

Here, $\sqrt{-g} = a^3(t)$, thus

$$\frac{1}{a^3}\left[-\partial_t\left(a^3\partial_t\right) + \frac{a^3}{a^2}\nabla^2\right] h_i{}^j(t,\vec{x}) = \left[-\partial_t^2 - 3\frac{\dot{a}}{a}\partial_t + \frac{1}{a^2}\nabla^2\right] h_i{}^j(t,\vec{x}) = 0 \tag{46}$$

and if we Fourier decompose to the modes $h_k(t)$ as in (40), assuming isotropy for now,

$$\left[-\partial_t^2 - 3\frac{\dot{a}}{a}\partial_t + \frac{1}{a^2}(-k^2)\right] h_k(t) = 0. \tag{47}$$

It is useful though, to work in conformal time η defined as $dt = ad\eta$. Now the metric is $g_{\mu\nu} = a^2(\eta)\eta_{\mu\nu}$ and (47) becomes

$$h_k''(\eta) + 2\frac{a'}{a}h_k'(\eta) + k^2 h_k(\eta) = 0 \tag{48}$$

where $h' = \frac{dh}{d\eta} = a\dot{h}$. The equation is easily solvable under the change of variable to

$$\begin{aligned}\psi_k(\eta) &= a(\eta)h_k(\eta)\\ \psi_k' &= a'h_k + ah_k'\\ \psi_k'' &= a''h_k + 2a'h_k' + ah_k''\end{aligned}$$

which eventually gives

$$\psi_k'' + \left[k^2 - \frac{a''}{a}\right]\psi_k = 0 \tag{49}$$

We can recognize the above equation as a *parametric oscillator*, i.e. an oscillator whose eigen-frequency varies with time. Let us denote the time dependent part of the coefficients with $U(\eta) = \frac{a''(\eta)}{a(\eta)}$, which, as a function of conformal time, depends on the dominant equation of state.

A crude qualitative analysis comes from distinguishing between *sub-Hubble* ($k^2 \gg U(\eta)$) and *super-Hubble* modes ($k^2 \ll U(\eta)$). The name sub-Hubble implies that the mode's wavelength is much shorter than the Hubble radius, which, in a simple de Sitter paradigm is obvious, since $a = \frac{-1}{H_I\eta}$ and $U(\eta) = 2/\eta^2$ so that sub-Hubble now means $k_{phys} = k/a \gg H_I$, or $a/k \ll R_H$. The sub-Hubble modes evolve as

$$\psi_k \propto \frac{1}{\sqrt{2k}}e^{\pm ik\eta} \tag{50}$$

whereas for the super-Hubble modes

$$\psi_k \propto a\left[D_k + C_k\int\frac{d\eta}{a^2}\right] \tag{51}$$

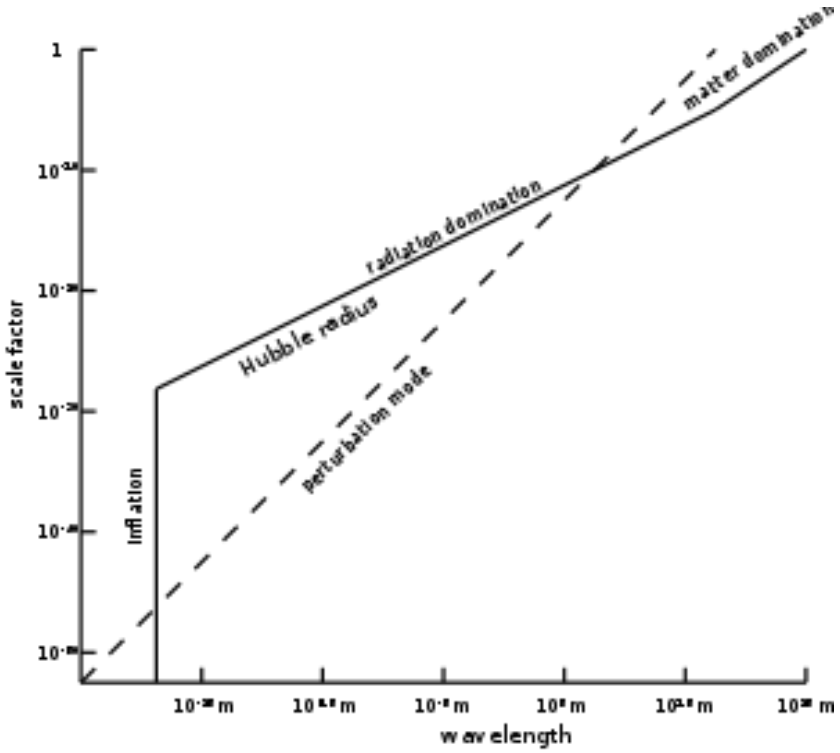

Figure 1: The way tensor modes of different wavelengths exit and re-enter the Hubble radius in a de Sitter inflationary paradigm. (Source : *en.wikipedia.org*)

There is a significant difference between the two which is clear when going back to $h_k = \psi/a$:

$$h_k \propto \frac{1}{\sqrt{2k}a} e^{\pm ik\eta} \quad , \quad k^2 \gg U(\eta) \tag{52}$$

$$h_k \propto C_k + D_k \int \frac{d\eta}{a^2} \quad , \quad k^2 \ll U(\eta) \quad , \tag{53}$$

where the second relation can be derived directly from (48), if the last term is neglected, leading to $h'(\eta) = Ca^{-2}(\eta)$. The two solutions need to match at intermediate scales, i.e. $k/a \approx H$ but the problem can also be treated exactly as we shall see in section 3.2.1.

Here we can see that the sub-Hubble modes are suppressed as the Universe expands by the factor $1/a$, while the super-Hubble mode amplitude behaves asymptotically as constant. This means that we effectively have a relative amplification of the modes that remain outside the Hubble radius during inflation with respect to the sub-Hubble wave modes and all physical lengths. After inflation and during radiation era these amplified modes may re-enter

the Hubble radius, as shown in figure 1, since now the equation of state gives $a \propto \eta$ and $U = 0$, thus turning into propagating gravitational waves.

$$\psi_k(\eta) = A_k \sin k\eta + B_k \cos k\eta \quad \text{or} \quad \psi_k(\eta) = \alpha_k e^{-ik\eta} + \beta_k e^{ik\eta} \tag{54}$$

Energy density

We can now find the energy density by averaging over $\dot{h}\dot{h}$ as mentioned in section 3.1, with $\dot{h} = \frac{\psi'}{a^2} - \frac{\psi}{a^2}\frac{a'}{a}$, so

$$\left\langle \dot{h}_{ij}\dot{h}_{ij} \right\rangle = \frac{1}{a^4}\left\langle \psi'_{ij}\psi'_{ij} - 2H\psi_{ij}\psi'_{ij} + H^2\psi_{ij}\psi_{ij} \right\rangle \approx \frac{1}{a^4}\left\langle \psi'_{ij}\psi'_{ij} \right\rangle \tag{55}$$

for $k/a \gg H$, so in terms of sub-Hubble Fourier modes,

$$\begin{aligned} \left\langle \psi'_{ij}(x)\psi'_{ij}(x) \right\rangle_V &= \frac{4}{V}\int d^3x \frac{d^3\vec{k}d^3\vec{k}'}{(2\pi)^3}\psi'_k\psi'_{k'}e^{-i(\vec{k}+\vec{k}')\vec{x}} \\ &= \frac{4}{V}\int \frac{d^3\vec{k}d^3\vec{k}'}{(2\pi)^3}(2\pi)^3\delta(\vec{k}+\vec{k}')\psi'_k\psi'_{k'} \\ &= \frac{16\pi}{V}\int_0^{+\infty} dk k^2 \psi'_k\psi'^*_k \end{aligned} \tag{56}$$

where we have used the polarization tensors to contract the indices $\epsilon^P_{ij}\epsilon^{ij}_P = 4$ and $\int d\hat{k} = 4\pi$. So for free waves of the form (54) the expected value of ρ_{gw} averaged over a period of oscillation will give

$$\langle \psi'_k\psi'^*_k \rangle_T = \frac{k^2}{2}\left(|\alpha_k|^2 + |\beta_k|^2\right) \tag{57}$$

$$\Rightarrow \rho_{gw} = \frac{1}{4G_N a^4 V}\int dk k^4 \left(|\alpha_k|^2 + |\beta_k|^2\right) \tag{58}$$

$$\Omega_{gw} = \frac{1}{\rho_c}\frac{d\rho_g w}{d\ln f} \propto k^3 \langle \psi'_k\psi'^*_k \rangle \tag{59}$$

It remains to be seen what coefficients of gravitational waves α_k and β_k are derived after the end of the inflationary epoch. This calculation is very sensitive to the scenario specifics and as a first example we will derive for de Sitter inflation, however unrealistic it may be.

3.2.1 de Sitter inflation

In the de Sitter case, the scale factor conformal time dependence during inflation is $a = -\frac{1}{H_I\eta}$ for $-\infty < \eta < \eta_I$, where η_I denotes the end of inflation

and the beginning of radiation era. The parametric oscillator ((49)) for $\frac{a''}{a} = \frac{2}{\eta^2} = 2H_I^2 a^2$ (H_I is constant) will give the 2nd order differential equation

$$\psi_k'' + \left[k^2 - \frac{2}{\eta^2}\right] = 0 \tag{60}$$

which can be solved exactly by means of Hankel functions giving

$$\psi_k(\eta) \propto \left[1 - \frac{i}{k\eta}\right] e^{-ik\eta} \quad , \quad \eta < \eta_I \tag{61}$$

This is an exact solution for equation (60) which can be derived as follows. First we rewrite (60) making the ansatz

$$\psi_k(\eta) = \sqrt{-\eta} y(-k\eta) \quad , \tag{62}$$

which yields :

$$\begin{aligned} \psi_k'(\eta) &= -\frac{1}{2\sqrt{-\eta}} y(-k\eta) - \sqrt{-\eta} k y'(-k\eta) \\ \psi_k''(\eta) &= -\frac{1}{4}(-\eta)^{-3/2} y(-k\eta) + \frac{k}{\sqrt{-\eta}} y'(-k\eta) + \sqrt{-\eta} k^2 y''(-k\eta) \quad . \end{aligned} \tag{63}$$

Now (60) becomes

$$\begin{aligned} &\sqrt{-\eta} k^2 y''(-k\eta) + \frac{k}{\sqrt{-\eta}} y'(-k\eta) - \frac{1}{4}(-\eta)^{-3/2} y(-k\eta) \\ &\qquad + k^2 \sqrt{-\eta} y(-k\eta) - 2(-\eta)^{-3/2} y(-k\eta) = 0 \\ &\Rightarrow \quad (-k\eta)^2 y''(-k\eta) + (-k\eta) y(-k\eta) + \left[(-k\eta)^2 - \frac{9}{4}\right] y(-k\eta) = 0 \end{aligned} \tag{64}$$

which turns out to be a Bessel function of the form:

$$x^2 y''(x) + x y'(x) + \left[x^2 - \alpha^2\right] y(x) = 0 \quad , \tag{65}$$

with $\alpha = \frac{3}{2}$. Solutions of half-integer (n-1/2)-Bessel equations are given in an analytic form as the first and second *Hankel functions* :

$$H_{n-1/2}^{(1),(2)}(x) = \sqrt{\frac{2}{\pi x}} i^{\mp n} e^{\pm ix} \sum_{k=0}^{n-1} \frac{(n+k-1)!}{k!(n-k-1)!} \left(\frac{\pm i}{2ix}\right)^k \quad , \tag{66}$$

which in our case, for $n = 2$ will be

$$\begin{aligned} H^{(1)}_{3/2}(-k\eta) &= -\sqrt{\frac{2}{-k\eta\pi}}e^{-ik\eta}\sum_{k=0}^{1}\frac{(1+k)!}{k!(1-k)!}\frac{i^k}{(-2k\eta)^k} \\ &= -\sqrt{\frac{2}{-k\eta\pi}}e^{-ik\eta}\left[1-\frac{i}{k\eta}\right] \end{aligned} \tag{67}$$

and $H^{(2)}_3/2$ its complex conjugate. These are the solutions for $y(-k\eta)$ and returning to $\psi_k(\eta)$ via (62) we get the equivalent of plane wave solutions

$$\begin{aligned} \psi^{(1)}_k(\eta) &= -\sqrt{\frac{2}{k\pi}}e^{-ik(\eta-\eta_I)}\left[1-\frac{i}{k\eta}\right] \\ \psi^{(2)}_k(\eta) &= -\sqrt{\frac{2}{k\pi}}e^{ik(\eta-\eta_I)}\left[1+\frac{i}{k\eta}\right] \quad . \end{aligned} \tag{68}$$

The general solution will be a linear combination of the two, i.e. $\psi_k = c_1\psi^{(1)}_k + c_2\psi^{(2)}_k$ and meets the condition that at very small scales we get a wave-like behavior, however the normalization imposed by the Wronskian [4] constraints the coefficients to $|c_1|^2 - |c_2|^2 = 1$. Towards the end of inflation, the perturbations also need to restrict to positive frequency waves, thus setting the coefficient of the second solution to zero. This stems from the fact that the vacuum "selects" this particular solution as that of lowest energy, namely the *Bunch-Davies vacuum*.

Of course we will ultimately have to match the above solution for the inflationary era, along with its derivative, to the solutions (54) for radiation dominated era (RD) at some time $\eta = \eta_I$ that denotes the end of inflation.

$$\psi_k(\eta) = \alpha_k e^{-ik(\eta-\eta_I)} + \beta_k e^{ik(\eta-\eta_I)} \tag{69}$$

There will be the two following matching conditions that will define the RD coefficients :

$$\psi_k(\eta_I) = \alpha_k + \beta_k = \frac{1}{\sqrt{2k}}\left(1-\frac{i}{k\eta_I}\right) \tag{70}$$

and

$$\begin{aligned} \psi'_k(\eta_I) = -ik\alpha_k + ik\beta_k &= \left[\frac{-ik}{\sqrt{2k}}\left(1-\frac{i}{k\eta_I}\right) + \frac{i}{k\sqrt{2k}}\frac{1}{\eta_I^2}\right] \\ \Rightarrow \quad \beta_k - \alpha_k &= \left[\frac{1}{\sqrt{2k}}\left(\frac{i}{k\eta_I}-1\right) + \frac{1}{k^2\sqrt{2k}\eta_I^2}\right] \end{aligned} \tag{71}$$

adding (70) and (71) will give the amplitude coefficients

$$\begin{aligned}\beta_k &= \frac{1}{2\sqrt{2}k^{5/2}\eta_I^2} \\ \alpha_k &= \frac{1}{\sqrt{2k}}\left[1 - \frac{i}{k\eta_I} - \frac{1}{2k^2\eta_I^2}\right],\end{aligned} \tag{72}$$

which, according to (58) will lead to a coincidentally k-independent "flat" spectrum, that today (redshifted) looks like [3]

$$h_0^2\Omega_{gw} \approx 4 \times 10^{-14}\left(\frac{H_I}{6 \times 10^{-5} M_{Pl}}\right)^2. \tag{73}$$

It is worth noting the particle interpretation of the amplification process. If we consider the linearized gravity as a free field theory of the graviton spin-2 field, we can say that when the transition from Inflation to RD takes place, we have to match states in different Fock spaces, built on the different vacua of the two epochs, which we can denote $|0\rangle^I$ and $|0\rangle^{II}$. Each epoch is filled with a number of gravitons to which we can assign bosonic creation and annihilation operators $b_P^{I,II}(\vec{k}), b_P^{I,II\dagger}(\vec{k})$, which act on their vacua respectively as usual.

$$b_P^{I,II}(\vec{k})|0\rangle_{I,II} = 0 \tag{74}$$

Now we can express the graviton field as a superposition of particles in the canonical bosonic form

$$h_{ij}^E = \sqrt{16\pi G_N}\sum_P \int \frac{d^3\vec{k}}{(2\pi)^3}\frac{1}{\sqrt{2k}}\left[b_P^E(\vec{k})h_k^E(\eta)\epsilon_{ij}^P(\hat{k})e^{i\vec{k}\vec{x}} + h.c.\right], \tag{75}$$

where $E = I, II$. In order to make this matching between h^I and h^{II} we have to perform a *Bogoliubov transformation* which will give the coefficients of Fock space I as a combination of Fock space II and vice versa. This is actually what is done semi-classically with α and β above. If one carries out the calculation [5] one can find a relation between the expectation values of the two number operators, $N_k^E = b_P^{E\dagger}(\vec{k})b_P^E(\vec{k})$ which shows how the graviton field is amplified by a factor of

$$N_k^{II} = N_k^I\left[1 + 2|\beta_k|^2\right] + |\beta_k|^2. \tag{76}$$

[3] In fact the exact approach would involve a recent MD era resulting to a f^{-2} scaling at the low frequency end of the spectrum. This reflects the fact that modes in this band entered the Hubble radius during MD, when H scales differently.

3.2.2 Slow-roll inflation

A less simple yet more realistic inflationary paradigm which also solves the "graceful exit" problem of de Sitter inflation, is *slow-roll* inflation. In this case, inflation is driven by a scalar field ϕ that, under a potential $V(\phi)$, satisfies a special set of slow-roll conditions : $\dot{\phi} \ll V(\phi)$ and $|\ddot{\phi}| \ll |3H\dot{\phi}|$.

The significant difference in terms of GW wave spectra comparing to the de Sitter case comes from the fact that in slow-roll the Hubble radius is not constant during inflation but slowly decreases as ϕ rolls down the potential towards the minimum. This means that the solution obtained by the matching conditions will *not* be scale invariant, thus resulting to a k-dependent spectrum. This happens in the same way as the different scaling of ultra-low frequencies in de Sitter inflation caused by a change in $H(t)$ when going to matter era. Ultimately the spectrum acquires a small tilt of $n_T = -\frac{M_{Pl}^2}{(8\pi)}\left(\frac{\bar{V}'}{\bar{V}}\right)^2$ which also does not raise our hopes for detection. On the contrary the tilt is found to be negative which makes it even worse. The quantity $\bar{V}'$ that appears above is the value of the inflaton potential derivative at the time when today's Hubble scale crossed the inflation's Hubble radius.

3.3 Inflaton Decay and Preheating

The above calculations can be extended to a more general case of strong time dependent field inhomogeneities that source gravitational waves after inflation. Such a process, called *preheating*, involves a set of scalar fields $\{\phi_a\}$ with a stress-energy tensor

$$T_{\mu\nu} = \partial_\mu\phi_a\partial_\nu\phi_a - g_{\mu\nu}\left(\frac{1}{2}g^{\rho\sigma}\partial_\rho\phi_a\partial_\sigma\phi_a + V(\phi_a,\ldots)\right) \tag{77}$$

Some of the fields are coupled to the inflaton and are significantly amplified inhomogeneously as it decays. We only consider sub-Hubble modes to be strong enough. The TT part of the above stress-energy tensor will be the one to source the gravity waves and only the first term will contribute significantly at sub-Hubble scales. So the perturbations will be sourced as

$$\psi''_{ij\vec{k}}(\eta) + k^2\psi_{ij\vec{k}}(\eta) = 16\pi G_N a T_{ij}^{TT}(\eta,\vec{k}) \tag{78}$$

where we Fourier transformed to $T_{ij}(\vec{k})$:

$$T_{ij}^{TT}(\vec{k}) = \Pi_{ij,lm}(\hat{k})\int\frac{d^3\vec{p}}{(2\pi)^{3/2}}p_l p_m\phi_a(\vec{p})\phi_a(\vec{k}-\vec{p}) \tag{79}$$

Starting from a time η_i when no gravity waves are present in sub-Hubble scales, and thus including the initial conditions $h_{ij}(\eta_i) = h'_{ij}(\eta_i) = 0$, the

Green's function solution with the above source will yield

$$\psi_{\vec{k}}(\eta) = \frac{16\pi G_N}{k}\int_{\eta_i}^{\eta} d\eta' \sin\left[k(\eta-\eta')\right] a(\eta') T_{\vec{k}}^{TT}(\eta') \tag{80}$$

and the conformal time derivative

$$\psi'_{\vec{k}}(\eta) = 16\pi G_N \int_{\eta_i}^{\eta} d\eta' \cos\left[k(\eta-\eta')\right] a(\eta') T_{\vec{k}}^{TT}(\eta') \tag{81}$$

where we have hidden the spatial indices i, j in the polarization tensors since we only deal with TT parts.

After preheating, when the sources eventually vanish at some time η_f, the Universe is believed to enter radiation era, so we return to the free streaming solutions of (54), so for $\eta \geq \eta_f$ the solution is

$$\psi_{\vec{k}}(\eta) = A_{\vec{k}} \sin\left[k(\eta-\eta_f)\right] + B_{\vec{k}} \cos\left[k(\eta-\eta_f)\right] \tag{82}$$

and

$$\psi'_{\vec{k}}(\eta) = A_{\vec{k}} k \cos\left[k(\eta-\eta_f)\right] - B_{\vec{k}} k \sin\left[k(\eta-\eta_f)\right]. \tag{83}$$

What is left now to be done is to match the solutions at the time of transition from sourced to free field $\eta = \eta_f$. This will give the coefficients:

$$\begin{aligned} A_{\vec{k}} &= \frac{16\pi G_N}{k}\int_{\eta_i}^{\eta_f} d\eta' \cos\left[k(\eta_f-\eta')\right] a(\eta') T_{\vec{k}}^{TT}(\eta') \\ B_{\vec{k}} &= \frac{16\pi G_N}{k}\int_{\eta_i}^{\eta_f} d\eta' \sin\left[k(\eta_f-\eta')\right] a(\eta') T_{\vec{k}}^{TT}(\eta') \end{aligned} \tag{84}$$

when matching $h'(\eta_f)$ and $h(\eta_f)$ respectively (or in this case, $\psi'(\eta_f)$ and $\psi(\eta_f)$).

As discussed in the previous section, the resulting energy density (59) will be given by

$$\begin{aligned} \rho_{gw} =& \frac{1}{16\pi G_N V a^4}\int d\hat{k} dk k^4 \left(\left|A_{\vec{k}}\right|^2 + \left|B_{\vec{k}}\right|^2\right) \\ =& \frac{(16\pi G_N)^2}{16\pi G_N V a^4}\int d\hat{k} dk k^2 \left\{\left|\int_{\eta_i}^{\eta_f} d\eta' \cos\left[k(\eta_f-\eta')\right] a(\eta') T_{\vec{k}}^{TT}(\eta')\right|^2 \right. \\ &\left. + \left|\int_{\eta_i}^{\eta_f} d\eta' \sin\left[k(\eta_f-\eta')\right] a(\eta') T_{\vec{k}}^{TT}(\eta')\right|^2 \right\} \end{aligned} \tag{85}$$

and we conclude by noting that

$$\begin{aligned} \Omega_{gw}(k) \propto \frac{d\rho_{gw}}{d\ln k} = k\frac{d\rho_{gw}}{dk} = \frac{16\pi G_N}{V a^4} k^3 \int d\hat{k} \times \\ \left\{\left|\int_{\eta_i}^{\eta_f} d\eta' \cos\left[k(\eta_f-\eta')\right] a(\eta') T_{\vec{k}}^{TT}(\eta')\right|^2 + \left|\int_{\eta_i}^{\eta_f} d\eta' \sin\left[k(\eta_f-\eta')\right] a(\eta') T_{\vec{k}}^{TT}(\eta')\right|^2 \right\}. \end{aligned} \tag{86}$$

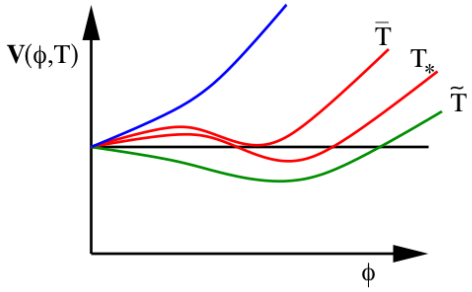

Figure 2: During a 1st order phase transition, the second well forms in the effective potential as the temperature drops ($\bar{T}$). In a second-order transition or a smooth crossover there symmetry is broken with no bubble nucleation since the old vacuum is now a local maximum ($\tilde{T}$).

One may consider the regime of sufficiently small frequencies, where the k-dependence comes only from the factor k^3 and the sinusodials and sources vary too slowly to give any scaling contribution, so $\Omega_{gw} \propto k^3$. In another intermediate regime (where source's k-independence still holds) the cos and sin integrals give a $1/k$ factor, thus resulting to a spectrum of $\Omega_{gw} \propto k$.

Further computations involve taking the ensemble average for the stochastic source $T^{TT}_{\vec{k}}$ as defined in (79) and tracking the spectral evolution up to the present time, and are carried out in [6].

3.4 Phase Transitions

As the Universe expanded and cooled down a sequence of phase transitions occurred at times when the temperature dropped below some characteristic critical value (usually some mass scale like the Higgs for the electroweak (EW) case). First order phase transitions may consist a source of gravitational radiation.

Let us consider such a transition driven by an effective potential $V(\phi, T)$ of a field ϕ. In high temperatures, the universe is in a metastable "symmetric" vacuum phase. As the temperature drops, a new potential well is formed which eventually becomes lower and more favorable then the initial minimum. In a 1st order phase transition a new "true" vacuum emerges in the effective field potential, separated from the old "false vacuum" by a potential barrier, that prevents the universe from making the transition instantaneously and leaves it trapped in the false vacuum state. But the transition will eventually take place, sooner or later depending on the height of the barrier, and this will happen only via quantum tunneling.

In the beginning small areas randomly distributed throughout the whole space will enter the new vacuum state and small bubbles of true vacuum will be nucleated. The latent heat left over after the transition, which amounts to the energy difference between false and true vacuum, will be transformed into bubble walls as kinetic energy, resulting in their expansion, and also reheat the primordial plasma. There are two ways in which gravitational waves can be produced from the above process. The first kind of source comes from the collisions of the expanded bubbles. When the walls of different bubbles meet each other they collide in relativistic speeds and an enormous amount of energy is released. The creation and expansion of bubbles in random sites intrinsically breaks the homogeneity and isotropy of the Universe during the transition from one vacuum state to another. In a strong first-order transition, the surfaces of collision, as shown in figure 3, anisotropic as it is, may have enough quadrupole moment to comprise a strong source of gravitational waves. A convenient form for the stress-energy tensor of the bubbles will be given by the following Fourier transformed

$$T_{ij}(\vec{k}) = \frac{1}{2\pi}\int_0^\infty dt e^{ikt}\left[\sum_{n=1}^{N} e^{-i\vec{k}\vec{x}_n}\int_{S_n} d\Omega \int_0^R dr r^2 e^{-i\vec{k}\vec{x}} T_{ij}(r,t)\right] \tag{87}$$

where we summed over the bubble surfaces, S_n and more specifically, the portion of each surface that remains uncollided at the time. Detonating bubble surfaces [7] expand at supersonic speeds, so collision regions do not affect the expansion of the uncollided walls. The radial integral for a single bubble of radius R will give

$$\int_0^R dr r^2 T_{ij}(r,t) = \frac{1}{3}R^3\kappa(\alpha)\epsilon\hat{x}_i\hat{x}_j \quad , \tag{88}$$

where $\kappa(\alpha)$ is the fraction of the vacuum energy ϵ that goes to collective bubble motion (kinetic energy of the walls e.g. $\kappa = 1$ for vacuum bubbles). The production of GWs is related to the quadrupole part of the source via the TT projection and the radiated energy in GWs will be

$$\frac{dE}{dkd\Omega} = 2G_N k^2 \Pi_{ij,lm}(\hat{k}) T^*_{ij}(\vec{k}) T_{lm}(\vec{k}) \quad . \tag{89}$$

The second kind of source comes from the reheated primordial plasma, in which turbulent eddies may appear, emitting gravitational radiation that can be as intense as the one coming from the wall collisions (or even more).

The spectrum coming from such a first-order phase transition has been first calculated numerically by Kosowsky, Kamionkowski and Turner in the early 90's, and is characterized by a peak frequency, which mainly depends on

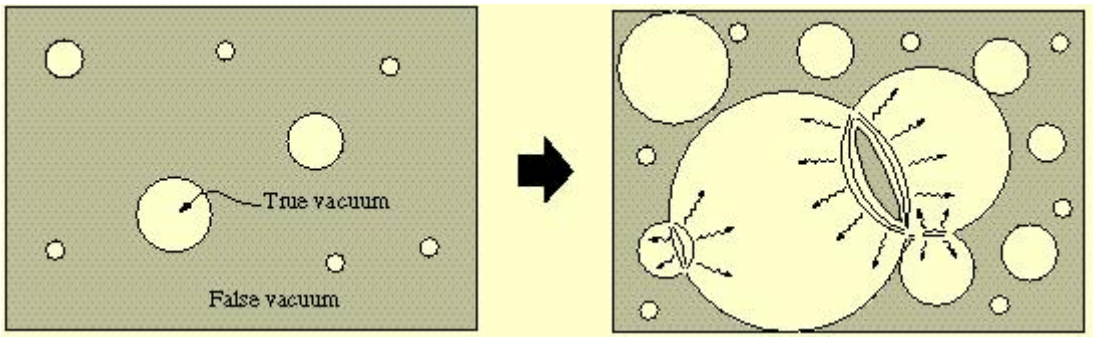

Figure 3: Bubble nucleation, bubble expansion and collisions. (Source : *http://www.damtp.cam.ac.uk/user/gr/public/cs_home.html*)

the temperature when the transition takes place. More specifically, a rough approximation for the peak frequency from bubble collision is given by the formula:

$$f_{max} \approx 5.2 \times 10^{-8} \left[\frac{\beta}{H_*}\right] \left[\frac{kT_*}{1GeV}\right] \left[\frac{g_*}{100}\right]^{1/6} Hz \tag{90}$$

which will give a peak at $4 \times 10^{-3} Hz$ (within the LISA band) for the case of a transition at a scale of the order $kT_* \approx 10^2 GeV$ as in the Standard Model EW transition.

The latest numerical calculations [8] show that the spectrum rises as f^3 for low frequencies and decreases as f^{-1}. According to these results, a GW spectrum strong enough to be detected within the sensitivity of future detectors (BBO) is still a possibility, as shown in figure 4 in contradiction to the original approach. Recently progress has been also made in an analytical approach to GW's from bubble collisions [9] which however is still under dispute. Two are the important parameters which determine the generated GW background. The parameter α gives a measure of the difference in the energy density between the two vacua, while the parameter β characterizes the bubble nucleation rate per unit volume.

$$\alpha = \frac{E_{f.v.}}{aT_*^4} \quad , \quad \Gamma = \Gamma_0 e^{\beta t} \tag{91}$$

The bubble nucleation will not result in a Universe in true vacuum until the expansion rate of the bubbles is of the order of the Hubble rate of expansion. If the Universe kept expanding faster than the true vacuum bubbles then it would be trapped in the false vacuum forever.

Naturally β also gives a rough estimate of the peak frequency $\beta \approx 2\pi f_{max}$ and also the duration of the phase transition $\beta^{-1} = \Gamma/\dot{\Gamma} = \tau$. Of course the whole spectrum underwent a certain redshift as discussed before. I will only

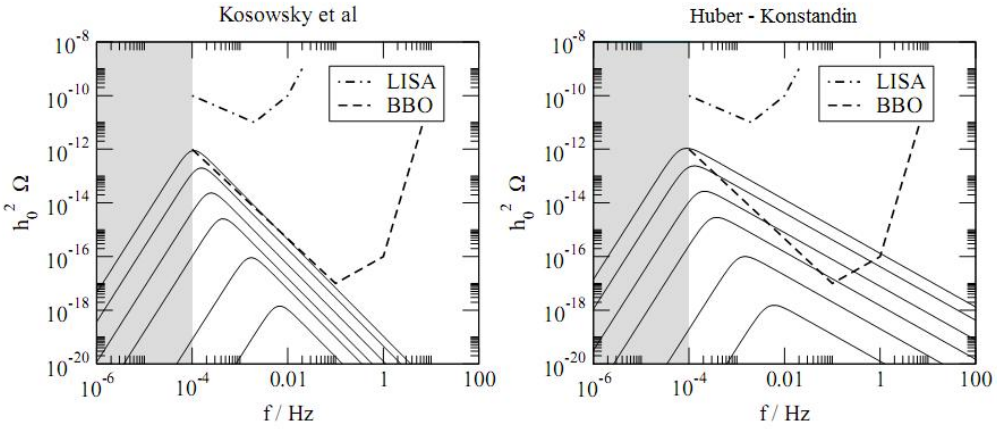

Figure 4: Comparison of several GW spectra for different values of α. In the second model a less steep fall-off slope is apparent. Adapted from [8].

present here the result of the calculations made by Kosowsky, Turner and Watkins [10], that derived the amplitude of the spectrum at the peak

$$\Omega_{gw}(f_{max})h_0^2 \approx 1.1 \times 10^{-6}\kappa^2 \left(\frac{H_*}{\beta}\right)^2 \left(\frac{\alpha}{1+\alpha}\right)^2 \left(\frac{v_b^3}{0.24+v_b^3}\right) \left(\frac{g_*}{100}\right)^{-1/3}, \tag{92}$$

where v_b is the bubble wall velocity in units of c. A strongly first-order transition needed requires $\alpha \to \infty$ and $\beta \to \infty$.

Nevertheless, all the above calculations are made in the context of rather speculative scenarios, none of which is proven to have actually happened. There are at least two well known phase transitions that is believed to have occurred during the thermal history of the Universe, namely the QCD phase transition and the EW phase transition. The QCD transition corresponds to the time when baryonic matter went from the quark-gluon plasma state to the confined state that we more or less observe today. However it has been shown that the QCD transition was not first order, but rather a smooth crossover, as predicted by today's experimental values.

In the Standard Model, the EW phase transition is also a crossover, according to the experimental restrictions for the Higgs mass to be above $114GeV$ (larger than the W mass). Even so, we can still expect other models in particle physics to give us a first-order EW transition, like for example SUSY. The Minimal Supersymmetric Standard Model, or MSSM provided that it comes with a sufficiently light *stop* $(105 - 165GeV)$ does give first-order, but theoretical calculations of thermal corrections are not so much in favor of this scenario, since the m_{stop} is not allowed to be low enough to give

a strong GW spectrum [11]. We then resort to the Next to Minimal Supersymmetric Standard Model (nMSSM) which is also quite appealing for other reasons, like providing a mechanism for baryogenesis. In the SUSY case, if a background is detected, we could in principle discriminate among variations of the model with different Higgs sectors. On the other hand we can also look for phase transitions at the GUT scale, which will give us a spectrum detectable by the Advanced LIGO detectors.

3.5 Cosmic Strings

A stochastic GW background can also be produced by a network of cosmic strings. Cosmic strings are topological defects generated via the Kibble mechanism during a phase transition when a spontaneous symmetry breaking occurs. If the broken vacuum manifold M has a nontrivial $n = 1$ homotopy group $\pi_1(M) \neq \mathbf{1}$ cosmic strings will form. These are one-dimensional massive objects (hence the name "string") of extraordinary linear mass densities. The characteristic quantity is the mass-per-unit-length denoted by μ and can reach typical values as high as $10^{22} gr/cm$ if the formation takes place at GUT scales $\sim 10^{16} GeV$.

In an extended network cosmic strings may cross either each other or themselves, forming kinks and small loops, the latter being detached from the main body of the string, while the former change the topology of the network. The string tension is remarkably strong, equal to its mass per unit length, and so it is expected that cosmic strings will vibrate at relativistic speeds and decay by emitting gravitational radiation. In fact small loops will decay much faster, nearly as fast as the time needed for light to travel across its diameter.

A very interesting statistical property of cosmic string networks, discovered by Vilenkin in the early 90's, says that at any given time, a Hubble sized volume contains a constant number of strings passing through it and a large number of small strings that are constantly decaying and replaced by newly formed ones. Loops are formed in a variety of sizes and will radiate in varying frequencies as they shrink. Further study of string evolution by Vilenkin, Shellard, Caldwell and Allen has predicted a spectrum relatively flat with a small bump at low frequencies, as shown in figure 6. However, most cosmic strings scenarios are disfavored or even ruled out by recent evidence, including the msec pulsar bound discussed below.

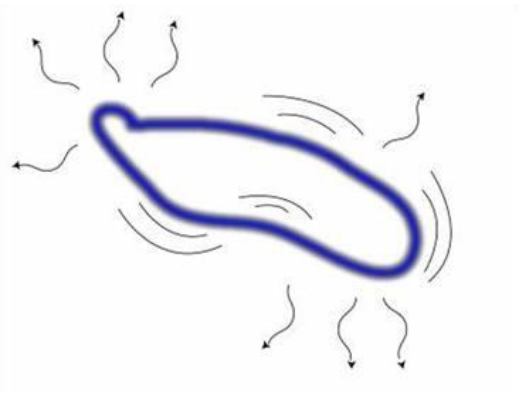

Figure 5: A decaying relativistically vibrating loop emits gravitational radiation. Source : *http://www.damtp.cam.ac.uk/user/gr/public/cs_home.html*

3.6 Other stochastic backgrounds

Apart from the causal mechanisms discussed above, cosmologists have come up with a rich variety of scenarios, most of which originate from superstring cosmologies. We previously saw that the standard inflationary models fail to give an ascending spectrum and a detectable signature. But this is not always the case. I will quickly mention some of the interesting cosmological models that leave us a hope for detection.

3.6.1 Pre-Big-Bang scenario

This is one of the String Cosmology scenarios that involve the dynamics of a dilaton field φ, the kinetic energy of which drives the inflation. The scale factor in (49) is now replaced by $\tilde{a} = e^{-\varphi/2}a$. The big bang singularity is replaced overridden and replaced with a "would be big bang singularity" stage which is still not fully understood. Before this stage, a phase of accelerated expansion (or contraction) at negative times took place, which extends to $t \to -\infty$. The main characteristic of this superinflation is a non-constant expansion rate $\dot{H} > 0$, which again results to a non-flat spectrum, this time ascending as

$$\Omega_{gw} = g_0^2 \left(\frac{H_*}{H_0}\right)^2 \left(\frac{a_*}{a_0}\right)^4 \left(\frac{f}{f_*}\right)^3, \tag{93}$$

where g_0 is the string coupling today, $f_* \sim 10^10 Hz$ and $*$ denotes the end of superinflation. This gives an strongly positive slope $n_T = 3$, but the characteristic values are expected to give a peak at the GHz region (which has to be under the BBN bound) and the spectrum overshoots the sensitive regions of our detectors. Also, for the ultra-low frequencies of the CMBR

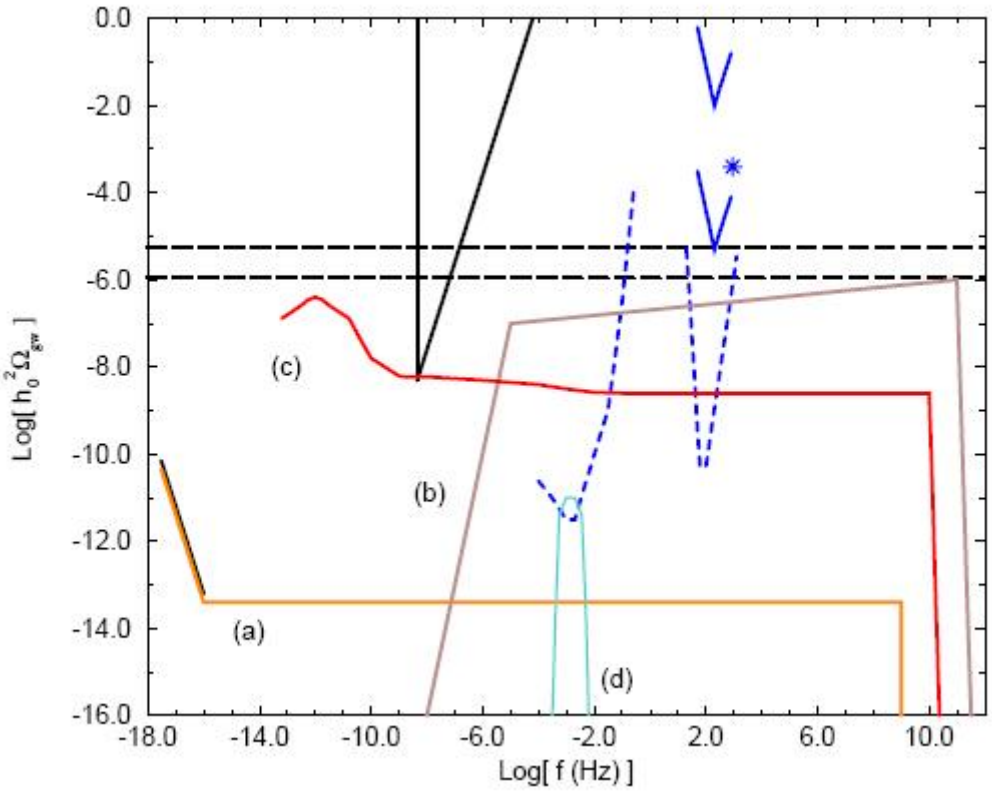

Figure 6: Spectra coming from several early Universe production mechanisms in comparison with bounds and detector sensitivities. a) Standard inflation (de Sitter, slow-roll), b) String Cosmologies, c) Cosmic Strings, d) first-order EW Phase Transition. Adapted from [12]

measurements, this scenario gives rather negligible contributions, so if tensorial contribution is detected by the successors of COBE, this idea will have to be ruled out. However the details of the calculations are far from being complete at least until we have some theoretical calculations for the Planck scale.

3.6.2 Brane World scenarios

This is another interesting String Theory originated scenario influenced by brane-world ideas. Our Universe comprises one of the two branes of the model the other of which is "hidden" and the dilaton field φ can be interpreted as the distance between the two branes. Here the big bang singularity is also eliminated and the Universe pre-exists, undergoing an accelerated con-

traction. The phases that the Universe undergoes close to $\eta = 0$ is initially a phase with $a \sim (-\eta)^{\epsilon}$, where ϵ is small (slow contraction), followed by a superinflationary phase as in the previous section with the power jumping from ϵ to 1/2 The end result will be a spectrum of perturbations which will have a slope $n_T = 2 + 2\epsilon$ for modes that became super-Hubble during the first phase and $n_T = 3$ for the ones that became super-Hubble during superinflation. Again this scenario can be ruled out by CMBR measurements as in the PBB case.

3.6.3 Quintessence

This scenario includes an epoch dominated by a new type of source stiffer than radiation, but with a non-standard equation of state, which is named "quintessence". After inflation, when the field ϕ has rolled down the potential to $\phi \sim -M_{Pl}$, it drives a phase of expansion by means of its kinetic energy, with $a \sim \sqrt{\eta}$. The final result will be a linearly scaling spectrum, i.e. slope $n_T = 1$ as a correction for the frequency band that includes modes that became super-Hubble during quintessential inflation and re-entered the Hubble radius during this kinetic phase. This spectrum is quite promising for detection since in some versions of its parameters, the ascending part may fall within the sensitivity range of the advanced LIGO detectors.

4 Bounds

This is the part of the story when experimental evidence restrict our ambitious GW stochastic background calculations, even if these evidence to not come directly from gravitational wave detectors. In this sense, one can distinguish between two types of experimental bounds, namely direct and indirect and we are unlucky enough to have both, the latter being the most difficult to overcome.

Our direct bounds come from all GW detectors that ever operated up to today, since none of them ever had the sensitivity to detect a single gravitational wave, not to mention a stochastic background. However, the relatively narrow frequency band of ground based interferometers and, even worse, resonant bar detectors, makes it difficult for us to derive conclusions about the stochastic background spectrum as a whole.

The indirect bounds on the other hand cover a totally different range of frequencies as shown below. The most important indirect bounds come from the Big Bang Nucleosynthesis calculations, millisecond pulsars and CMBR measurements carried out first by COBE and later on by WMAP. In this

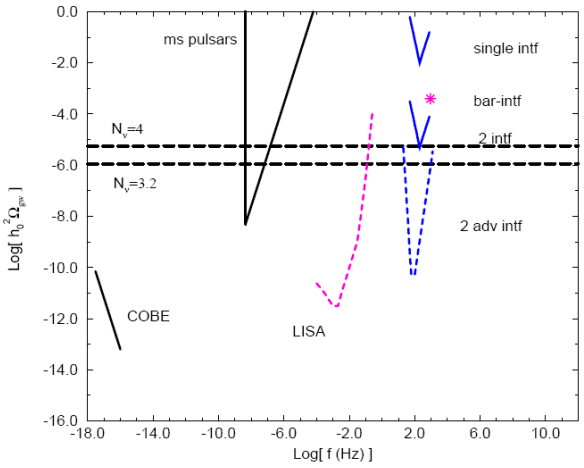

Figure 7: The three basic bounds BBN, msec Pulsars and COBE, and the current and future (dotted) detection experiments. Adapted from [12].

section we will overview each of them separately. In figure 7 we include all the important bounds available today, both direct and indirect, along with the expected sensitivities of the future detectors LISA and Advanced LIGO.

4.1 The BBN bound

The Big Bang Nucleosynthesis calculations provide us with a very successful prediction for the abundances of light elements in the Universe. The bulk of todays Deuterium, Helium isotopes ^3He and ^4He, as well as ^7Li are coming from the primordial nucleosynthesis, the outcome of which is extremely sensitive to the coupling constants of all fundamental interactions and the expansion rate of the Universe H. A change in H would result to a change of the *freeze-out* temperature when nucleosynthesis takes place and would in turn change the ratio of proton and neutron production and, consequently, the light element abundances, thus spoiling our so precious results.

It is now easy to make the connection between the BBN results and the GW spectrum. GW's were not taken into account in the original calculations. Since H is directly related to the energy densities via the Friedmann equations, if the total energy density of gravitational waves Ω_{gw} at the time of nucleosynthesis was too high, then H and $T_{freezeout}$ would also become too high etc. This restriction on the **total** energy density is expressed to good approximation by the final result for the total GW energy density today:

$$\int_{f=0}^{f=\infty} d(\log f) h_0^2 \Omega_{gw}(f) \leq 5.65 \times 10^{-6} \Delta N_\nu \tag{94}$$

This is a result in terms of the "effective number of neutrino species" defined as $N_\nu = (\rho_{rel} - \rho_\gamma)/\rho_{\nu,th}$ at the time of nucleosynthesis, where ρ_{rel} accounts for photons, three species of neutrinos and other relativistic contribution, including GWs. This extra contribution is denoted by ΔN_ν and is a number smaller than 1, with 95% confidence [13, 14]. Two such bounds are shown in figure 7. Unless the spectrum of the stochastic background shows a strong peak in a narrow band and is much smaller in the rest of the spectrum, which is highly unlikely, the BBN bound imposes a restriction across the whole range of frequencies of roughly

$$h_0^2 \Omega_{gw} \leq 5 \times 10^{-6}. \tag{95}$$

It is also important to point out that this bound does not apply to a stochastic background of Astrophysical origin and GWs coming from post-BBN times in general.

4.2 Millisecond Pulsars

Another constraint on today's Universe abundance in gravitational waves comes from the very accurate timing of msec pulsars, the first of which, PSR B1937+21, was discovered in 1937. These are objects that emit a signal of remarkably high precision and were observed carefully for almost a decade, giving a pulse period as precise as 16 digits long.

This property provides us with a natural gravitational wave detector, since passing GWs would cause a very small variation in the measured period of the pulse, proportional to the GW amplitude. This can be understood as a pulse coming from the pulsar being successively redshifted and blueshifted as a GW passes between us and the source. The duration of observation defines the maximum period of the measurable variation, and thus a minimum frequency for the GW bound of $\sim 10^{-8} Hz$. The bound extends naturally to the frequency of the msec pulse ($\sim 10^3 Hz$), above which the "detector" is rather insensitive. Ultimately, the extremely small size of the timing errors $\Delta t/t \leq 10^{-16}$ at a maximum sensitivity frequency of $f_* = 4.4 \times 10^{-9}$ gives an amplitude bound of

$$h_0^2 \Omega_{gw}(f_*) < 4.8 \times 10^{-9} \tag{96}$$

at a confidence level of 90%

4.3 COBE and the Sachs-Wolfe effect

Finally, a very important bound is the one coming from detailed measurements of the anisotropies of the Cosmic Microwave Background Radiation.

The COsmic Background Explorer (COBE) satellite measured the black body temperature fluctuations for the whole 4π solid angle and found a maximum value of fluctuations of the order $\Delta T/T \leq 10^{-5}$. The anisotropy was also measured, in terms of the multipole coefficients and the smallness of this anisotropy suggests a bound on Ω_{gw} at ultra-low frequencies $10^{-18} - 10^{-16} Hz$.

The above connection has been made by virtue of the Sachs-Wolfe effect. The general concept is the following; the CMBR spectrum comes from the photons' last scattering surface which corresponds to a redshift of $z_{LSS} \sim 10^3$ (about 350.000 years after the big bang). Super-Hubble modes of metric tensor perturbations at that time would comprise gravitational potential wells and hills resulting to a certain redshift or blueshift of the photons as they enter these regions. As modes re-enter the Hubble radius and continue as GWs in later times of RD or MD, this frequency shift will be observable to us today as an anisotropy in the CMBR black body temperature. The explicit calculation predicts a bound for the amplitude *today*

$$h_0^2 \Omega_{gw}(f) < 7 \times 10^{-11} \left(\frac{H_0}{f} \right) \quad , \quad 3 \times 10^{-18} Hz < f < 10^{-16} Hz \qquad (97)$$

Scalar perturbations can also source anisotropies but, depending on the inflationary model, are considered to be subdominant.

At the upper edge of its range COBE imposes the strongest bound so far: 7×10^{-14} @ $f \sim 10^{-16} Hz$, which has great impact on the whole range of almost scale invariant spectra, predicted by many inflationary scenarios. If the spectrum is almost flat, then a strong bound at any frequency would imply almost as strong bounds at all frequencies.

5 Detection and Experiments

One would not describe the history of Gravitational Wave Detection as a success story, but rather a story of discomfort and great unease of experimental physicists. The first experimentalist to claim to have detected a gravitational wave was the pioneer in the field of GW detectors, J. Weber. The first resonant bar detector was designed by him in the early 60s and became operational in 1965. During the first months of its operation a strong signal was detected which could not be interpreted as noise in any way. In a series of other more advanced experiments that took place during the following years, Weber saw a few more such unlikely events, however he was the only one to do so. Thus up to today no direct detection of GWs has been confirmed and the only convincing evidence that we have supporting their existence are indirect evidence coming from the measurements of binaries' power loss which

perfectly matches the theoretical predictions. The new interferometric type of GW detectors are much more promising than the old resonant bars, they have a few orders of magnitude higher sensitivity and cover a much wider range of (lower) frequencies. The sensitivity is further enhanced when the detectors work correlated.

5.1 Correlated detectors

The signal from a GW stochastic background is expected to be far from strong. However, it seems that by correlating the signal measured by two or more detectors, which work simultaneously in remote locations and have an uncorrelated noise, we can dig out a very tiny signal buried under a relatively strong noise. This technique was first studied by Michelson in the late 1980s and further developed by Flanagan and Christensen in the '90s. Correlated detectors can give a combined sensitivity that may reach several orders of magnitude higher than the one obtained by each detector separately.

Suppose that the signal S_i seen by each detector can be split in two parts; a pure gravitational wave signal s_i and a background noise n_i, where i labels the detector, so

$$S_i(t) = s_i(t) + n_i(t), \tag{98}$$

and suppose that the signal-to-noise ratio $(SNR)_i^2 = \frac{\langle s_i^2(t)\rangle}{\langle n_i^2(t)\rangle}$ is quite low ($\ll 1$). In principle we cannot separate the signal from the background noise as it is. However, we can use the fact that the GW signal is correlated in the two detectors (both detectors measure the same passing GW with a small time delay depending to their distance) [4], while the noise signal is totally random and uncorrelated. Let us define the very simplified version of the correlation signal

$$S = \langle S_1, S_2\rangle \equiv \int_{-T/2}^{T/2} S_1(t)S_2(t)dt, \tag{99}$$

where T is the time interval of correlated operation and for a weak signal

$$\begin{aligned} S &= \langle s_1, s_2\rangle + \langle s_1, n_2\rangle + \langle n_1, s_2\rangle + \langle n_1, n_2\rangle \\ &\approx \langle s_1, s_2\rangle + \langle n_1, n_2\rangle \quad , \end{aligned} \tag{100}$$

since the cross terms are uncorrelated and much smaller than the uncorrelated noise-noise term.

[4] Here for simplicity we have made the additional assumption that the distance between the detectors is very small compared to the wavelength of the GW to be measured, so that the detectors are oscillating in phase. A typical value of this for ground based detectors gives $f < 100Hz$

A consequence of the above is that if we turn both detectors on and wait for a long period of time T, then the signal correlation will linearly grow, while the noise correlation will behave as a 1-dim random walker:

$$\begin{aligned} \langle s_1, s_2 \rangle &\propto |s(f)|^2 \Delta f T \\ \langle n_1, n_2 \rangle &\propto |n(f)|^2 \sqrt{\Delta f T} \end{aligned} \tag{101}$$

from which we conclude that the minimum detectable amplitude of energy density $\Omega_{gw}(f) \propto |s(f)|^2$, will drop as

$$\Omega_{gw,det} \propto \frac{|n(f)|^2}{\sqrt{\Delta f T}}. \tag{102}$$

So in principle if one waits long enough, one can find a signal no matter how small it is compared to the noise. The actual convoluted signal uses an "optimal filter" $Q(t-t')$ which is determined by more advanced calculations and also takes into account the relative orientation of the interferometers' arms, which stand on different planes.

5.2 Ground based interferometers

The construction of the first generation of large scale interferometers took place in the early 2000s with the two LIGO detectors in the US (Louisiana and Washington) the VIRGO in Pisa, Italy, and the smaller GEO600 in Hannover, Germany and TAMA300 in Mitaka, Japan.

They all basically operate under the same principles. A laser beam is emitted and split in two, each of which travels along a different arm of the interferometer and back. The interference pattern shows in extraordinary precision variations in the relative armlengths hopefully enough to indicate a passing of a GW. The precision needed in order to detect GWs in an order of km long interferometer is a real challenge to current technology, since it may reach scales as small as the size of a proton. Therefore a very important task is noise reduction. Noise can be either seismic, in the form of ground vibrations, or even thermal, coming from the microscopic random motion of the several parts of the detector (e.g. the mirrors' surface molecules) which for this reason are cooled to ultra-low temperatures. In order to deal with ground noise, the mirrors are hanged from wires that are connected via a series of seismic filters to a very well stabilized platform.

Single interferometers operate in the range between $1Hz$ and a few kHz and can measure a spectrum of minimum amplitude $h_0^2\Omega_{gw} \sim 10^{-2}$ which is rather high. However, pairs of combined detectors, like LIGO-LIGO, LIGO-VIRGO etc., correlated as discussed in the previous section can reach after a

year of integration a minimum amplitude sensitivity of $\sim 5 \times 10^{-6}$. However this is still not enough for detection.

The second generation of enhanced sensitivity interferometers is expected to improve the current sensitivity by at least a factor of 10. This includes the advanced LIGO detectors, usually referred to as LIGO 2 which should be operational by 2014. It is believed that LIGO 2 will detect GWs, maybe even on a daily basis.

5.3 LISA

The Laser Interferometer Space Antenna is the first GW interferometer that will be sent to outer space. It consists of three identical spacecrafts which will form a huge triangle the sides of which will be the arms of the interferometer, of length $\sim 5 \times 10^6 km$ (as long as 100 times the Earth's perimeter). This is a joint project of NASA and ESA and it has been planned for more than a decade. The current estimated time of launch is between 2018 and 2020 in the most optimistic scenario.

LISA's resonant frequency band ranges from $10^{-5} Hz$ to $1 Hz$ and cannot be covered by any other earth-bound detector due to ground noise. Each spacecraft will carry the same equipment including a 1 Watt laser and a 30cm telescope, and will operate both as a mirror and as a detector/transmitter thus producing 3 independent signals and transforming LISA to effectively more than one detectors. The equipment may not be capable of measurements as precise as the ones made by the ground-based detectors but the final sensitivity of the experiment is a few orders of magnitude higher than the LIGOs'. This happens not only due to reduced noise, but also because the stochastic wave strain falls of as $f^{-3/2}$ which actually means that detectors working in a lower frequency band require much less precision for the same outcome in sensitivity.

The orbit that LISA is planned to follow is that of the Earth's revolution around the Sun, following our planet in a 20 deg lag. The triangle will have a relative tilt of 60 deg with respect to the ecliptic plane and will perform a rolling motion along its orbit. The GW detection will be looked for as a variation in LISA's armlengths, all distances being measured in a precision of picometers, with respect to the spacecrafts' proof masses. The proof mass is a small test mass placed inside a perfectly isolated cavity, so that it performs an undisturbed free fall in the Sun's potential, free from noise like cosmic radiation, solar wind etc. During LISA's lifetime, the armlengths will undergo a small precession as it orbits around the Sun. However the timescale of these length variations will be long enough to be recognizable and calibrated out.

LISA's sensitivity in stochastic GW radiation is expected to reach $h_0^2\Omega \sim 10^{-12}$ and it is almost certain that a large population of Astrophysical sources will directly be detected. Unfortunately LISA will not be able to correlate to any ground base detector, but only to itself, mainly because of the different frequency band of operation. LISA's quest is scheduled to last 2-3 years and a test project, LISA-pathfinder will be launched beforehand (scheduled in 2010) in order to check the details of the orbit, but also the feasibility of the project. A successor of LISA is already being scheduled, under the name "Big Bang Observer" (BBO) and will consist of 4 LISA-like triangles a pair of which will form an hexagram.

6 Conclusions

Even though Gravitational Waves have quite stubbornly insisted to remain undetected for almost 50 years of scientific effort, theory has made progress on its own both in the field of Astrophysics and that of Cosmology. Various Cosmological models predict different forms of stochastic spectra some of which are possibly detectable by the forthcoming experiments of advanced sensitivity. The mechanisms in question occurred in the early Universe either as varieties of inflationary scenarios, or effects of phase transitions. However, as optimistic as we can be about future detectors, it will still remain a challenge to separate a stochastic spectrum of Cosmological origin from the overwhelming Astrophysical stochastic background coming from the abundance of binaries in our vicinity.

References

[1] S. Weinberg, *Gravitation and Cosmology: Principles and Applications of the General Theory of Relativity*. Gravitation and Cosmology: Principles and Applications of the General Theory of Relativity, by Steven Weinberg, pp. 688. ISBN 0-471-92567-5. Wiley-VCH , July 1972., July, 1972.

[2] E. E. Flanagan and S. A. Hughes, "The basics of gravitational wave theory," *New J. Phys.* **7** (2005) 204, `arXiv:gr-qc/0501041`.

[3] L. P. Grishchuk, "The Amplification of Gravitational Waves and Creation of Gravitons in the Isotropic Universe," *Nuovo Cim. Lett.* **12** (1975) 60–64.

[4] J. F. Koksma, "Decoherence of cosmological perturbations. On the classicality of the quantum universe," Master's thesis, ITP Utrecht University, 2007.

[5] A. Buonanno, "Gravitational waves from the early universe," arXiv:gr-qc/0303085.

[6] J. F. Dufaux, A. Bergman, G. N. Felder, L. Kofman, and J.-P. Uzan, "Theory and Numerics of Gravitational Waves from Preheating after Inflation," *Phys. Rev.* **D76** (2007) 123517, arXiv:0707.0875 [astro-ph].

[7] M. Kamionkowski, A. Kosowsky, and M. S. Turner, "Gravitational radiation from first order phase transitions," *Phys. Rev.* **D49** (1994) 2837–2851, arXiv:astro-ph/9310044.

[8] S. J. Huber and T. Konstandin, "Gravitational Wave Production by Collisions: More Bubbles," *JCAP* **0809** (2008) 022, arXiv:0806.1828 [hep-ph].

[9] C. Caprini, R. Durrer, and G. Servant, "Gravitational wave generation from bubble collisions in first-order phase transitions: an analytic approach," *Phys. Rev.* **D77** (2008) 124015, arXiv:0711.2593 [astro-ph].

[10] A. Kosowsky, M. S. Turner, and R. Watkins, "Gravitational radiation from colliding vacuum bubbles," *Phys. Rev.* **D45** (1992) 4514–4535.

[11] R. Apreda, M. Maggiore, A. Nicolis, and A. Riotto, "Supersymmetric phase transitions and gravitational waves at LISA," *Class. Quant. Grav.* **18** (2001) L155–L162, arXiv:hep-ph/0102140.

[12] M. Maggiore, "Stochastic backgrounds of gravitational waves," arXiv:gr-qc/0008027.

[13] M. Giovannini, H. Kurki-Suonio, and E. Sihvola, "Big bang nucleosynthesis, matter-antimatter regions, extra relativistic species, and relic gravitational waves," *Phys. Rev.* **D66** (2002) 043504, arXiv:astro-ph/0203430.

[14] G. Mangano, G. Miele, S. Pastor, and M. Peloso, "A precision calculation of the effective number of cosmological neutrinos," *Phys. Lett.* **B534** (2002) 8–16, arXiv:astro-ph/0111408.

[15] A. Buonanno, M. Maggiore, and C. Ungarelli, "Spectrum of relic gravitational waves in string cosmology," *Phys. Rev.* **D55** (1997) 3330–3336, arXiv:gr-qc/9605072.

[16] S. M. Carroll, "Lecture notes on general relativity," arXiv:gr-qc/9712019.

[17] R. M. Wald, *General relativity*. Chicago, University of Chicago Press, 1984, 504 p., 1984.

[18] S. Dodelson, *Modern cosmology*. Modern cosmology / Scott Dodelson. Amsterdam (Netherlands): Academic Press. ISBN 0-12-219141-2, 2003, XIII + 440 p., 2003.

[19] R. Apreda, M. Maggiore, A. Nicolis, and A. Riotto, "Gravitational waves from electroweak phase transitions," *Nucl. Phys.* **B631** (2002) 342–368, arXiv:gr-qc/0107033.

[20] E. Coccia, F. Dubath, and M. Maggiore, "On the possible sources of gravitational wave bursts detectable today," *Phys. Rev.* **D70** (2004) 084010, arXiv:gr-qc/0405047.

[21] M. Maggiore, "Gravitational waves and fundamental physics," arXiv:gr-qc/0602057.

[22] B. Allen, "The stochastic gravity-wave background: Sources and detection," arXiv:gr-qc/9604033.

[23] D. Langlois, "Early Universe: inflation and cosmological perturbations," arXiv:0811.4329 [gr-qc].

[24] C. Cutler and K. S. Thorne, "An overview of gravitational-wave sources," arXiv:gr-qc/0204090.

[25] M. Gasperini and G. Veneziano, "The pre-big bang scenario in string cosmology," *Phys. Rept.* **373** (2003) 1–212, arXiv:hep-th/0207130.

[26] A. Nicolis, "Relic gravitational waves from colliding bubbles and cosmic turbulence," *Class. Quant. Grav.* **21** (2004) L27, arXiv:gr-qc/0303084.

[27] B. F. Schutz, "Low-frequency sources of gravitational waves: A tutorial," arXiv:gr-qc/9710079.

[28] G. F. R. Ellis and H. van Elst, "Cosmological models," *NATO Adv. Study Inst. Ser. C. Math. Phys. Sci.* **541** (1999) 1–116, arXiv:gr-qc/9812046.

[29] M. Maggiore, "Gravitational wave experiments and early universe cosmology," *Phys. Rept.* **331** (2000) 283–367, arXiv:gr-qc/9909001.

[30] A. Buonanno, "Gravitational waves," arXiv:0709.4682 [gr-qc].

[31] C. Ungarelli and A. Vecchio, "High energy physics and the very-early universe with LISA," *Phys. Rev.* **D63** (2001) 064030, arXiv:gr-qc/0003021.

[32] L. F. Abbott and D. D. Harari, "GRAVITON PRODUCTION IN INFLATIONARY COSMOLOGY," *Nucl. Phys.* **B264** (1986) 487.

[33] L. P. Grishchuk, "Discovering Relic Gravitational Waves in Cosmic Microwave Background Radiation," arXiv:0707.3319 [gr-qc].

[34] W. Zhao, D. Baskaran, and L. P. Grishchuk, "On the Road to Discovery of Relic Gravitational Waves: the TE and BB Correlations in the Cosmic Microwave Background," arXiv:0810.0756 [astro-ph].

[35] J. F. Dufaux, G. N. Felder, L. Kofman, and O. Navros, "Gravity Waves from Tachyonic Preheating after Hybrid Inflation," arXiv:0812.2917 [astro-ph].

[36] L. Kofman, A. D. Linde, and A. A. Starobinsky, "Towards the theory of reheating after inflation," *Phys. Rev.* **D56** (1997) 3258–3295, arXiv:hep-ph/9704452.

[37] C. J. Hogan, "Cosmological gravitational wave backgrounds," arXiv:astro-ph/9809364.

[38] A. Linde, "Particle physics and inflationary cosmology.," *Physics Today* **40** (1987) 61–68.

[39] K. Ichikawa, M. Kawasaki, and F. Takahashi, "Constraint on the Effective Number of Neutrino Species from the WMAP and SDSS LRG Power Spectra," *JCAP* **0705** (2007) 007, arXiv:astro-ph/0611784.

[40] S. J. Huber and T. Konstandin, "Production of Gravitational Waves in the nMSSM," *JCAP* **0805** (2008) 017, arXiv:0709.2091 [hep-ph].

[41] C. Caprini and R. Durrer, "Gravitational waves from stochastic relativistic sources: Primordial turbulence and magnetic fields," *Phys. Rev.* **D74** (2006) 063521, arXiv:astro-ph/0603476.

[42] C. Caprini, R. Durrer, and R. Sturani, "On the frequency of gravitational waves," *Phys. Rev.* **D74** (2006) 127501, arXiv:astro-ph/0607651.